Distinctive roles of translesion polymerases DinB1 and DnaE2 in diversification of the mycobacterial genome through substitution and frameshift mutagenesis.

Pierre Dupuy[1], Shreya Ghosh[2], Oyindamola Adefisayo[1,3], John Buglino[1], Stewart Shuman[2] and Michael Glickman[1,3,*]

[1]Immunology Program, Sloan Kettering Institute, New York, NY 10065, USA.

[2]Molecular Biology Program, Sloan-Kettering Institute, New York, NY 10065, USA.

[3]Immunology and Microbial Pathogenesis Graduate Program, Weill Cornell Graduate School, 1300 York Avenue, New York, NY 10065, USA

*To whom correspondence should be addressed. Tel: +1 646 888 2368; Fax: +1 646 422 0502 Email: glickmam@mskcc.org

ABSTRACT

Antibiotic resistance of *Mycobacterium tuberculosis* is exclusively a consequence of chromosomal mutations. Translesion synthesis (TLS) is a widely conserved mechanism of DNA damage tolerance and mutagenesis, executed by translesion polymerases such as DinBs. In mycobacteria, DnaE2 is the only known agent of TLS and the role of DinB polymerases is unknown. Here we demonstrate that mycobacterial DinB1 abets insertion and deletion frameshift mutagenesis in homo-oligonucleotide runs. DinB1 is the primary mediator of spontaneous -1 frameshift mutations in homo-oligonucleotide runs whereas DnaE2 and DinBs are redundant in DNA damage-induced -1 frameshift mutagenesis. DinB1 also promotes missense mutations conferring resistance to rifampicin, with a mutational signature distinct from that of DnaE2. These results highlight DinB1 and DnaE2 as drivers of mycobacterial genome diversification with relevance to antimicrobial resistance and host adaptation.

INTRODUCTION

Genomic integrity is constantly threatened by DNA damage arising from endogenous cell metabolism and exogenous environmental factors. DNA lesions, when not rectified by dedicated repair systems, can persist, block DNA replication, and induce lethal fork collapse. "Translesion DNA Synthesis" (TLS) is an ubiquitous tolerance pathway by which the blocked replicative polymerase is transiently replaced by an alternative DNA polymerase that traverses the lesion (Vaisman and Woodgate, 2017). In *E. coli*, DinB (Pol IV) and UmuDC (Pol V) are critical mediators of TLS (Fuchs and Fujii, 2013; Fujii and Fuchs, 2020). In vitro, DinB and UmuDC share common biochemical characteristics that facilitate their in vivo function, including low fidelity, low processivity, lack of proofreading activity, and ability to bypass a variety of lesions (Reuven et al., 1999; Tang et al., 1999; Wagner et al., 1999). In *E. coli*, the expression of *dinB* and *umuDC* is inducible by DNA damage through the SOS response pathway (Courcelle et al., 2001) and they respectively confer tolerance to alkylating agents and UV (Bjedov et al., 2007; Courcelle et al., 2005; Jarosz et al., 2006). Because of their intrinsic flexibility, TLS polymerases catalyze mutagenesis and play a key role in evolutionary fitness (Yeiser et al., 2002) or antibiotic resistance in bacteria (Boshoff et al., 2003) and carcinogenesis in eukaryotes (Sale, 2013). In *E. coli*, DinB and UmuDC are highly mutagenic, inducing substitution mutations as well as indels (Kato and Nakano, 1981; Kim et al., 1997, 2001; Napolitano et al., 2000; Steinborn, 1978; Wagner and Nohmi, 2000).

Mycobacterium tuberculosis (Mtb) is the causative agent of tuberculosis (TB), which kills 1.5 million of people annually (WHO, 2021). The major challenges impeding TB eradication efforts include the lack of short regimens of therapy, likely due to antibiotic tolerance mechanisms, and mutational antibiotic resistance (Nathan and Barry, 2015), which is a substantial global health problem (WHO, 2021). Mtb acquires antimicrobial resistance exclusively through chromosomal mutations, in contrast to the widespread mechanism of lateral gene transfer in other pathogens (Gillespie, 2002). Human macrophages, the natural habitat of Mtb, expose the bacterium to diverse stresses, many of which directly damage DNA (Darwin and Nathan, 2005; Ehrt and Schnappinger, 2009; Houghton et al., 2012; Naz et al., 2021; Stallings and Glickman, 2010). Mtb DNA repair pathways, in particular translesion polymerases, represent a promising and underexplored target for new TB drugs due to their role in survival within the host and in antimicrobial resistance

(Boshoff et al., 2003). However, the molecular pathways controlling chromosomal mutagenesis in mycobacteria are only partially understood. The replication fidelity of the Mtb chromosome is preserved by the proofreading function of the replicative polymerase DnaE1 that, when mutated, drastically increases mutation frequency (Rock et al., 2015). Mycobacteria do not encode UmuDC but rather another TLS polymerase, a paralogue of DnaE1 called DnaE2 (Cole et al., 1998; Erill et al., 2006). In Mtb, *dnaE2* expression is dependent on DNA damage response (Adefisayo et al., 2021; Boshoff et al., 2003). DnaE2 is involved in UV tolerance as well as UV-induced mutagenesis and also contributes to bacterial pathogenicity and the emergence of drug resistance (Boshoff et al., 2003; Warner et al., 2010). To date, DnaE2 is the only non-replicative polymerase known to contribute to chromosomal mutagenesis in mycobacteria.

Mycobacterial genomes encode several DinBs paralogs: two in Mtb (*dinB1*/*dinX*/Rv1537 and *dinB2*/*dinP*/Rv3056) and three in the non-pathogenic model *Mycobacterium smegmatis* (*dinB1*/MSMEG_3172, *dinB2*/MSMEG_2294/MSMEG_1014 and *dinB3*/MSMEG_6443) (Cole et al., 1998; Timinskas and Venclovas, 2019). In silico and experimental evidence indicates that DinB1, but not DinB2 nor DinB3, has a C-terminal β clamp binding motif and interacts directly with the β clamp in a heterologous organism (Kana et al., 2010). *M. smegmatis* DinB1, DinB2, and DinB3 are active DNA polymerases in vitro (Ordonez and Shuman, 2014; Ordonez et al., 2014). Initial characterization of a *dinB1dinB2* double mutant of Mtb, as well as the expression of the proteins in *M. smegmatis*, failed to identify a role in DNA damage tolerance, mutagenesis or pathogenicity in vivo (Kana et al., 2010).

Here we genetically investigate the contribution of mycobacterial TLS polymerases in DNA damage tolerance, antibiotic resistance, and mutagenesis. We show that DinB1 is highly mutagenic in vivo with a strong ability to incorporate substitution mutations conferring the resistance to rifampicin, one of the main drugs used to treat TB, and with a distinct mutagenic signature compared to DnaE2-catalyzed resistance mutations. We also demonstrate a previously unappreciated role for mycobacterial translesion polymerases in frameshift (FS) mutagenesis, with DinB1 and DnaE2 acting as the primary agents of spontaneous and UV-induced homo-oligonucleotide -1 FS mutagenesis in the mycobacterial chromosome.

RESULTS

Mtb DinB1 requires an N terminal extension for activity.

Although *M. smegmatis* DinBs all have vigorous polymerase activity in vitro (Ordonez and Shuman, 2014; Ordonez et al., 2014), indicating that these enzymes should be active in vivo, prior experiments (Kana et al., 2010) did not reveal an effect of Mtb *dinB1* or *dinB2* expression in *M. smegmatis* on either the frequency of rifampicin resistance, FS mutagenesis in homo-oligonucleotide runs, or growth. To examine this apparent discrepancy, we expressed *M. smegmatis dinB1* (*dinB1*^{Msm}) from an Anhydrotetracycline (ATc) inducible promoter (tet promoter) and measured bacterial growth. We found that the expression of *dinB1*^{Msm} in *M. smegmatis* caused a substantial growth defect and loss of viability (Figures 1A, B, and S1A) that was proportional to the level of inducer (Figure S1A, B). *dinB1*^{Msm} expression also triggered the DNA damage response, as evinced by an increase in the steady-state level of the RecA protein at 4 h post-induction by ATc (Figure 1C). However, the effect of DinB1 on growth was not due to activation of the DNA damage response as it was preserved in the Δ*recA* background (Figure S1C).

The effects of expression of *M. smegmatis dinB1* contrast with the lack of similar findings when the Mtb gene was expressed (Kana et al., 2010), despite an overall identity of the two proteins of 75% (Figure S1E). We confirmed the published results that expression of the Mtb *dinB1* gene (*dinB1*^{Mtb}) in *M. smegmatis* did not phenocopy *dinB1*^{Msm} (Figure 1D). However, we reanalyzed the annotation of the *dinB1* open reading frames from *M. smegmatis* and Mtb and found an alternative translational start codon fifteen nucleotides upstream of the annotated start codon of Mtb *dinB1* used in prior experiments (Figures 1E and S1E). Expression of this longer form of the Mtb DinB1 (*dinB1*$^{Mtb+5aa}$) impaired *M. smegmatis* growth (Figure 1D), suggesting that the first five amino acids of DinB1 are essential for in vivo activity. These results indicate that prior conclusions about lack of in vivo activity of Mtb DinB1 are attributable to expression of a truncated protein.

DinB1 competes with the replicative polymerase for interaction with the β clamp at the replication fork.

A catalytic dead mutant of *dinB1*^{Msm} (*dinB1*^{D113A}), which is unable to catalyze DNA synthesis in vitro (Ordonez et al., 2014), exacerbated growth and viability defects compared to the WT polymerase (Figures 1A and 1F). In contrast, expression of a *dinB1*^{Msm} mutant lacking its β clamp

binding domain (*dinB1*$^{\Delta\beta clamp}$), predicted to not interact with the replicative machinery, did not cause growth inhibition or cell death (Figures 1F and 1G). These results indicate that DinB1 interacts with the replicative machinery in vivo and competes with the replicative DNA polymerase at replication forks.

DinB1 is an error prone polymerase inducing antibiotic resistance through a characteristic mutagenic signature.

Because of the intrinsic flexibility required for lesion bypass, most translesion polymerases are error prone. To determine the mutagenic capability of mycobacterial DinB1 as well as its ability to induce antibiotic resistance, we measured the frequency of rifampicin resistance (rif^R), conferred by substitution mutations in the *rpoB* gene, in strains with temporally controlled expression of *dinB1*^{Msm}, *dinB1*^{Mtb}, or *dinB1*$^{Mtb+5aa}$. In the strains carrying the empty vector or the *dinB1*^{Mtb} plasmid, we respectively detected an average of 5.5 and 3.1 rif^R/10^8 CFU 16 h after inducer addition (Figure 2A). The expression of *dinB1*^{Msm} or *dinB1*$^{Mtb+5aa}$ increased the frequency of rif^R by 6- or 8-fold but the expression of *dinB1*$^{\Delta\beta clamp}$ had no effect, showing that an interaction between DinB1 and the replicative machinery is required for DinB1-dependent mutagenesis. We observed a similar induction of mutagenesis after *dinB1*^{Msm} expression in Δ*recA* and Δ*dnaE2* backgrounds (Figure S1D), showing that the effect of *dinB1* on mutation frequency is not the consequence of the DNA damage response or the previously defined role of DnaE2 in mutagenesis (Boshoff et al., 2003), further strengthening the conclusion that DinB1 is directly mutagenic.

To determine the mutation spectrum induced by DinB1, we sequenced the rifampicin resistance determining region (RRDR) of the *rpoB* gene (Figure 2B). In absence of *dinB1* expression, the majority of RRDR mutations were either G>A or C>T (37%) or A>G or T>C (28%), with a minority of other mutations. Expression of *dinB1*^{Msm} and *dinB1*$^{Mtb+5aa}$ strongly enhanced the relative proportion of A>G or T>C. The absolute frequency of these mutations was increased by 18- and 21-fold after *dinB1*^{Msm} and *dinB1*$^{Mtb+5aa}$ expression, respectively. Around 75% of *rpoB* mutations found after *dinB1* expression were in the second nucleotide of the His442 codon compared with 25% in control cells (Figure 2C and Table S2). The mutation was almost exclusively CAC>CGC (His>Arg) and its absolute frequency was increased 21- and 28-fold after *dinB1*^{Msm} and *dinB1* $^{Mtb+5aa}$ expression, respectively (Figure 2D and Table S2).

These results demonstrate that DinB1 is prone to induce mutations in vivo, with a characteristic mutagenic signature, A>G or T>C transition mutations, that contributes to rifampicin resistance at a specific codon in RpoB.

DnaE2 but not DinBs mediates stress-induced substitution mutagenesis.

The intrinsic mutagenicity of DinB1 demonstrated above supports a role for the enzyme in chromosomal mutagenesis in the absence of exogenous DNA damage. We next measured the relative contributions of mycobacterial TLS polymerases (DinBs and DnaE2) in spontaneous mutagenesis by characterizing *M. smegmatis* cells lacking *dnaE2*, all *dinBs*, or all known translesion polymerases (*dnaE2*+*dinBs*).

In the WT strain, we detected around 5 $rif^R/10^8$ CFU (Figure 3A) and 30% of *rpoB* mutations found in rif^R colonies were A>G or T>C, 27% were G>A or C>T, and the remainder distributed across other mutation types (Figure 3B). The deletion of TLS polymerases did not alter the frequency of rif^R or shift the proportion of mutation types found in the *rpoB* gene (Figures 3A and 3B), indicating that the activities of DnaE2 and DinBs are not the predominant mediators of substitution mutagenesis in the basal conditions tested.

By analyzing our recently published transcriptomic data (Adefisayo et al., 2021), we found that the expression of *dinB1*, *dinB3*, and *dnaE2* was induced by UV and ciprofloxacin in *M. smegmatis* whereas *dinB2* expression was unaffected (Figure S2). The expression level of *dinB1* and *dinB2* in UV-irradiated cells was not impacted by *recA* deletion (Figure S2). By contrast, UV-induction of *dinB3* and *dnaE2* expression was reduced in the Δ*recA* mutant, a result we confirmed by RT-qPCR (Figure S2).

We next investigated the relative contribution of DinBs and DnaE2 to stress-induced mutagenesis by measuring the frequency of rif^R in strains exposed to UV, hydrogen peroxide (H_2O_2) and methyl methanesulfonate (MMS). In the WT strain, we found 108-, 16-, and 24-fold increases of the rif^R frequency after treatment with UV, H_2O_2, and MMS, respectively (Figure 3A). All three mutagens increased the relative and absolute frequencies of G>A or C>T mutations in the RRDR whereas UV also enhanced A>C or T>G mutations and H_2O_2 increased G>C or C>G mutations (Figure 3B). UV- and H_2O_2-induced mutagenesis was DnaE2-dependent, declining by 10- and 4-fold in Δ*dnaE2* cells compared to WT, whereas MMS-induced mutagenesis was not impacted (Figure

3A). All types of UV- and H_2O_2-induced rif^R mutations were reduced by the *dnaE2* deletion (Figure 3B). In contrast, the *dinB123* deletion did not significantly decrease the mutation frequency in cells treated with UV, H_2O_2, and MMS or change the spectrum of mutation types (Figures 3A and 3B). The analysis of *rpoB* mutations incorporated by DnaE2 during oxidative stress (WT vs Δ*dnaE2*) revealed that, unlike DinB1, DnaE2 conferred rifampicin resistance by mutating diverse *rpoB* codons (Figure 3C and Table S2). Particularly, we found that the presence of DnaE2 increased the absolute mutation frequency in Ser447(TCG>TTG), Ser438(TCG>TTG), His442(CAC>TAC), His442(CAC>GAC), and Asn435(AAC>AAG), but not the DinB1 associated mutation His442(CAC>CGC).

These results show that DnaE2, but not DinBs, mediates UV- and H_2O_2-induced substitution mutagenesis with a distinct mutation spectrum from the DinB1 signature.

Redundancy of DinB1 and DnaE2 in tolerance to alkylation damage.

The mutagenic properties of DinBs are intimately linked to their flexibility in lesion bypass, a property that confers tolerance to agents that damage template DNA. We therefore investigated the role of mycobacterial TLS polymerases in DNA damage tolerance. A previous study did not identify a role for Mtb *dinB1* and *dinB2* in damage tolerance (Kana et al., 2010) but the possibility of redundancy between *dinB*s and *dnaE2* was not tested. The *M. smegmatis* Δ*dnaE2* Δ*dinB123* mutant was not more sensitive than the WT to H_2O_2 (Figure S3A) or ciprofloxacin (Figure S3B). As reported by Boshoff *et al*., we found that the Δ*dnaE2* deletion increased the sensitivity to UV (Figure S3C) and mitomycin C (Figure S3D) but we did not observe an additive effect caused by Δ*dinB123* deletion.

We next investigated the role of DnaE2 and DinBs in the tolerance to alkylation damage by testing the sensitivity of *M. smegmatis* TLS polymerase mutants to the chemical methylating agents MMS and methylnitronitrosoguanidine (MNNG). Using disc diffusion assays, we found that the Δ*dinB123* or Δ*dnaE2* mutants were not more sensitive than the WT strain to MMS but the loss of the four TLS polymerases in combination conferred severe sensitivity (Figure 4A), indicating substantial redundancy. We obtained similar results by plating serial dilutions of these strains on agar medium containing MMS (Figure S3F) and with disc diffusion using MNNG (Figure 4C). The Δ*dnaE2* Δ*dinB123* MMS and MNNG sensitivity was partially complemented by the introduction of an ectopic copy of $dnaE2^{Msm}$ or $dinB1^{Msm}$ but not $dinB2^{Msm}$ or $dinB3^{Msm}$ (Figures

4B, 4D, S3F, and S3G). The Δ*dnaE2* Δ*dinB123* sensitivity to MMS and MNNG was also complemented by an ectopic copy of *dinB1*^{Mtb} but not *dinB2*^{Mtb} (Figures 4B and 4D), indicating a conservation of DinB1 activities between fast- and slow-growing mycobacteria.

Finally, we measured the effect of loss of *dinB*s and *dnaE2* on tolerance to N^2-dG adducts. None of the translesion polymerase mutants was impacted in their tolerance to 4-nitroquinoline -1oxide (4-NQO) (Figure S3E). Whereas the Δ*dinB1,* Δ*dinB2*, and Δ*dnaE2* single mutants were slightly more sensitive than the WT strain to nitrofurazone (NFZ) (Jarosz et al., 2006), the Δ*dinB123* and Δ*dnaE2* Δ*dinB123* mutants were highly sensitive (Figure 4E). Ectopic expression of *dinB1*^{Msm}, *dinB3*^{Msm}, *dnaE2*^{Msm} or *dinB1*^{Mtb} in the Δ*dnaE2* Δ*dinB123* reversed the NFZ sensitivity (Figure 4F), reinforcing the substantial redundancy of translesion polymerases in mycobacteria for bypassing damage. These results reveal previously unrecognized roles for DnaE2 and DinB1 in the tolerance to genomic alkylation damage in mycobacteria and suggest a dominant role of DinB1 over the other mycobacterial DinBs in TLS.

DinB1 mediates -1 frameshift mutations.

The data above indicate that DinB1 catalyzes substitution mutations that confer resistance to antibiotics such as rifampicin or streptomycin by abolishing drug binding while maintaining the functionality of the essential antibiotic target. However, the diversity of mutational alterations of the chromosome that impact bacterial phenotypes includes not only substitutions, but chromosomal rearrangements, deletions, and FS mutations. Recently, FS mutagenesis has emerged as an important mechanism of genome diversification in mycobacteria (Gupta and Alland, 2021; Safi et al., 2019) but the agents of FS mutagenesis in mycobacteria are not known.

Translesion polymerases can introduce FS mutations during lesion bypass (Fujii and Fuchs, 2020; Vaisman and Woodgate, 2017), which prompted us to query the role of DinBs and DnaE2 in FS mutagenesis. To detect -1 FS mutations, we created a reporter system in which the chromosomal *leuD* gene carries a 2-base pair deletion in the second codon (*leuD*$^{-2}$), which confers leucine auxotrophy (Figure 5A). Reversion of this mutation by -1 or +2 FS confers leucine prototrophy (leu$^+$) which is selected on leucine free media. In WT cells, the reversion frequency was 5 leu$^+$/10^8 CFU (Figure 5B). Sequencing of *leuD* in leu$^+$ colonies revealed a -1 deletion in a run of 3T in almost half the revertants (44%). The other half had +2 addition (10%), >2-nucleotide insertion (7%), >2-nucleotide deletion (5%), or no mutation in *leuD* (32%) (Figure 5B and Table S3). The

expression of the inactive *dinB1*^{Mtb} did not increase leu^{+} frequency, but expression of *dinB1*^{Msm} or *dinB1*$^{Mtb+5aa}$ increased leu^{+} frequency 4- or 27-fold due to a dominant proportion of -1 FS in the homo-oligonucleotide run of 3T.

We then investigated the ability of DinB1 to incorporate +1 FS mutations using a *leuD* reporter with a one nucleotide deletion in the second codon (*leuD*$^{-1}$) (Figure S4A). In WT cells, the leu^{+} frequency was 1/10^{7} CFU but the mutations were mixed between +1 FS in *leuD* and an unexpected class of -1 FS mutations at the 3' end of the upstream *leuC* gene, which suppressed the native *leuC* stop codon and restored the reading frame of the *leuD* coding sequence to create a LeuC-LeuD fusion protein (Figure S4A). The expression of *dinB1*^{Msm} increased leu^{+} frequency by 16-fold but the sequencing of leu^{+} colonies revealed that *dinB1* expression exclusively catalyzed -1 FS at the 3' end of the *leuC* gene, with 97% of these mutations in a 3C run. These results reveal that DinB1 can promote -1 FS mutations in the mycobacterial genome and does so more efficiently than promoting +1 FS mutations.

DinB1 incorporates -1 FS and +1 FS in homo-oligonucleotide runs in vivo.

The location of the FS mutations in short homo-oligonucleotide tracts of *leuC* and *leuD* suggested that DinB1 may be a catalyst of FS mutagenesis in low complexity sequences. To more precisely measure the capability of DinB1 to incorporate -1 and +1 FS in homo-oligonucleotide runs in vivo and determine the effect of homomeric template sequence, we constructed integrative plasmids carrying a gene which confers resistance to kanamycin (*kan*) inactivated by the incorporation of 4T (*kan*::4T), 4C (*kan*::4C), 4G (*kan*::4G), 4A (*kan*::4A), 5T (*kan*::5T), 5G (*kan*::5G), or 5A (*kan*::5A) runs in the coding strand immediately 3' of the start codon (Figure 5A). These plasmids do not confer kanamycin resistance, but a deletion of one nucleotide (-1 FS) in the 4X run or +1 FS in the 5X run will restore the reading frame of *kan* allowing selection for kan^{R}.

We first measured the ability of DinB1 to incorporate -1 FS in homo-oligonucleotide runs by using the *kan*::4N constructs. We found between 5 and 18 kan^{R}/10^{8} CFU, depending on the run sequence, in strains carrying the empty vector and the vast majority kan^{R} colonies had -1 FS in the homo-oligonucleotide runs (Figures 5C, S4B, S4C, and S4D). Expression of *dinB1*^{Msm} enhanced -1 FS in runs of 4T, 4C, 4G, and 4A by 12-, 19-, 11-, and 3-fold, respectively. *dinB1*$^{Mtb+5aa}$ expression also increased -1 FS by 14- and 19-fold in 4T and 4C runs, respectively, but had no effect on runs of 4G or 4A.

By using the *kan*::5N constructs, we quantified the capacity of DinB1 to incorporate +1 FS in homo-oligonucleotide runs. Between 10 and 74 $kan^R/10^8$ CFU were detected in strains carrying the empty vector, depending on the nature of the run (Figures 5D, S4E, and S4F). We found +1 FS in the run of the majority of the sequenced kan^R colonies of all strains. Expression of *dinB1* increased the frequency of +1 FS localized in runs of 5T, 5G, and 5A by 3-, 6-, and 21-fold, respectively. $dinB1^{Mtb+5aa}$ expression also elicited +1 FS in the 5T (10-fold increase), 5G (3-fold increase), and 5A (5-fold increase) runs. Overall, these data reveal that mycobacterial DinB1 is a strong mediator of -1 FS and +1 FS in homo-oligonucleotide runs.

DinB1 can slip on homo-oligonucleotide runs in vitro.

To test if the DinB1 polymerase is prone to slippage on homo-oligomeric template tracts in vitro, we employed a series of 5' ^{32}P-labeled primer-template DNA substrates consisting of a 13-bp duplex with a 5'-tail composed of a run of four, six, or eight consecutive A nucleotides (A4, A6, A8) immediately following the primer 3'-OH terminus and flanked by three C nucleotides (Figure 5E). Reaction of a DNA polymerase with the A4, A6, and A8 primer-templates in the presence of only dTTP should, if the polymerase does not slip or mis-incorporate dTMP opposite the template nucleotide following the A run, allow for the addition of four, six, or eight dTMP nucleotides to the primer terminus. However, if the polymerase is prone to backward slippage, then the primer strand can recess and realign to the template to allow one or more additional cycles of dTMP addition. Whereas most of the primer extension events catalyzed by DinB1 on the A4, A6, and A8 templates in the presence of dTTP did indeed cease at the end of the A run (e.g., denoted by ▸ for the A4 reaction in Figure 5E), we consistently detected the synthesis of a minority product one nucleotide longer, consistent with a single slippage step mimetic of a +1 frameshift (Figure 5E). DinB1 displayed the same behavior when reacted with a series of DNAs in which the template strand tail comprised a run of four, six, or eight consecutive T nucleotides (T4, T6, T8) followed by three G nucleotides (Figure 5E). In presence of dATP, the majority of the primer extension events on the T4, T6, and T8 templates entailed 4, 6, and 8 cycles of dAMP addition, respectively. A +1 slippage product was also detected. The propensity to slip, defined as +1/[+1 plus ▸], increased progressively as the template T tract was lengthened from T4 (1%) to T6 (11%) to T8 (16%) (Figure 5E). The +1 products are unlikely to have arisen via addition of a 3'-terminal

mismatched dNMP, insofar as we could detect no extension of the 13-mer primer stands on the A6 and T6 templates when DinB1 was presented with the incorrect dNTP (Figure S5).

The finding that a DinB1 is capable of +1 slippage synthesis on a homo-oligomeric tract when the only dNTP available is that templated by the homo-oligomer does not reflect the situation in vivo where the polymerase will have access to the next correctly templated dNTP. To attempt to query whether provision of the next templated dNTP in vitro suppresses slippage, we included a dideoxy NTP (ddNTP): either ddGTP templated by the run of three C nucleotides following the A4, A6, and A8 tracts or ddCTP templated by the run of three G nucleotides flanking the T4, T6, and T8 tracts. Inclusion of the next templated ddNTP following the homo-oligomeric template tract was only partially effective in triggering conversion of the 17, 19, and 21 nt species to the respective ddG- or ddC-terminated 18, 20, and 22 nt products (Figure 5E). We considered several possibilities, including: (i) that DinB1 might disengage from the primer-template when the 5' tail comprising the template strand becomes shorter, and hence lose efficiency in adding opposite the third nucleotide from the 5' end of the template strand; or (ii) DinB1 is inherently feeble at using dideoxy NTPs as substrates; or (iii) DinB1 and the primer 3'-OH end can slip forward on the template run by a single nucleotide on the homo-oligonucleotide run (mimetic of a -1 FS) and this species is extended by ddNMP incorporation to yield a product that comigrates with the 17, 19, and 21 nt species. These issues were addressed by reacting DinB1 with the A6 and T6 primer-templates in the presence of various nucleotide substrates and combinations thereof. DinB1 catalyzed six steps of dTMP addition to the A6 template in the presence of dTTP and inclusion of dGTP elicited three further steps of dGMP addition opposite the 5'-terminal CCC element of the template strand (Figure S5), indicating that DinB1 is competent for fill-in synthesis. In the reaction with ddTTP only, a small fraction of the primer was elongated by the expect single nucleotide step showing that DinB1 is unable to efficiently utilize ddTTP as a substrate for correct templated addition. Similar results were obtained for the T6 primer-template (Figure S5). These results suggest that +1 slippage by DinB1 is dampened by the presence of the next correctly templated dNTP.

The question remains whether any of the residual 17, 19, and 21 nt species seen in Figure 5E represent -1 slips consistent with scenario (iii) above. In the case of the T tract templates, we see that the fraction of products that fail to be extended in the presence of ddCTP increases

progressively as the template tract lengthens from 4T (13% unextended) to 6T (34%) to 8T (48%). This result suggests a contribution of -1 slippage (rather than pure failure to incorporate ddC), the reasoning being that lengthening the template homo-oligonucleotide run is expected to enhance slippage but not impact DinB1's ability to incorporate ddNTPs.

DinB1 is the primary mediator of spontaneous -1 FS in runs of homo-oligonucleotides.

To determine the relative contribution of TLS polymerases in spontaneous FS mutagenesis, we measured the frequency of -1 FS in strains lacking *dnaE2* or *dinB*s using the *leuD*$^{-2}$ reporter (Figure 6A). The Δ*dinB2*, Δ*dinB3*, and Δ*dnaE2* deletions did not reduce the leu$^+$ frequency or the proportion of -1 FS detected in leu$^+$ colonies (Figure 6A and Table S3). In contrast, the leu$^+$ frequency decreased by 5-, 3-, and 5-fold in the Δ*dinB1,* Δ*dinB123* and Δ*dnaE2* Δ*dinB123* mutants, respectively, and the proportion of -1 FS mutations localized in the 3T run of *leuD* was also reduced. Expression of *dinB1* in the Δ*dinB1* strain restored both the WT leu$^+$ frequency and the proportion of -1 FS localized in the 3T run of *leuD* (Figure 6B and Table S3).

We extended these findings using the *kan*::4N reporters (Figures 6C, S6A, S6B, and S6C). Compared to WT, the kan^R frequency measured with the *kan*::4C reporter decreased by 9-, 9-, and 14-fold in the Δ*dinB1,* Δ*dinB123,* and Δ*dnaE2* Δ*dinB123* mutants, respectively, but we did not detect decrement in the Δ*dinB2*, Δ*dinB3,* and Δ*dnaE2* mutants (Figure 6C). The absolute frequency of -1 FS detected in the 4C run was reduced 54-fold in the Δ*dinB123* mutant. In contrast, there was no impact of *dinB1* deletion on the frequency of -1 FS mutation in 4T, 4G, or 4A runs (Figures S6A, S6B, and S6C). In Δ*dinB123* cells, -1 FS in the 4T run was reduced 4-fold but was unaffected in the 4G and 4C runs. Finally, we did not detect a significant impact of the TLS polymerase deletions on spontaneous +1 FS mutagenesis using the *kan*::5T, *kan*::5G or *kan*::5A reporters (Figures S6D, S6E, and S6F).

These results show that: (i) DinB1 is the dominant TLS polymerase involved in spontaneous -1 FS mutations in some homo-oligonucleotide runs; (ii) there is a redundancy between DinB1 and at least one other DinB for certain homopolymeric sequences; and (iii) endogenous levels of DinBs do not mediate spontaneous +1 FS mutations in unstressed cells.

DnaE2 is the primary mediator of UV-induced -1 FS mutagenesis.

Prior literature (Boshoff et al., 2003) as well as our data above (Figure S2) show that some mycobacterial TLS polymerases are DNA damage inducible, indicating that FS mutagenesis may be enhanced by DNA damage. To query the role of DNA damage in stimulating FS mutagenesis and the role of TLS polymerases in this process, we used the *leuD* and *kan* systems in conjunction with UV treatment. UV irradiation increased the frequency of leu^+ in the WT strain carrying the *leuD*$^{-2}$ reporter by 9-fold due to the induction of three main mutation types: -1 FS in the 3T run, -1 FS outside of the run, and base substitutions that in many cases created a new in-frame translational start codon that restored LeuD (Figure 7A and Table S3). The induction of the three mutation types was reduced in Δ*dnaE2* and Δ*dnaE2* Δ*dinB123* mutants. The residual UV-dependent increase of the -1 FS mutations in the *leuD* 3T run in the Δ*dnaE2* mutant was completely abolished in the Δ*dnaE2* Δ*dinB123* mutant, suggesting redundancy between DnaE2 and DinBs for damage-induced frameshifting.

We also measured the impact of UV on -1 FS using the *kan* reporters. In the WT strain carrying the *kan*::4T vector, irradiation increased the frequency of kan^R by 5-fold and 100% of the sequenced clones had a -1 FS in the homo-oligonucleotide run (Figure 7B). The -1 FS frequency was not reduced in either the Δ*dnaE2* or Δ*dinB123* mutants but decreased 5-fold in the Δ*dnaE2* Δ*dinB123* mutant. UV treatment also enhanced -1 FS in the 4C, 4G, and 4A runs in WT cells but not in the *dnaE2* mutant (Figures S7A, S7B, and S7C). 25% and 43% of the DnaE2-dependent mutagenic events detected with the *kan*::4G and *kan*::4A reporters, respectively, comprised -1 FS mutations located outside of the homo-oligonucleotide runs (Figures S7B and S7C), showing that the frameshifting activity of DnaE2 is not restricted to homo-oligonucleotide runs. Finally, although we detected a DnaE2-dependent increase of kan^R frequency in strains carrying *kan*::5T, *kan*::5G. or *kan*::5A reporters (Figures S7D, S7E, and S7F), these events were not due to FS mutagenesis and rather were nucleotide substitutions that created a new start codon.

These results reveal that DnaE2 is a major contributor to -1 FS mutations in response to DNA damage and that these FS are not restricted to homo-oligonucleotide runs. We also found that the DinBs have a redundant role with DnaE2 in -1 FS mutagenesis in response to DNA damage which differs depending on the sequence context.

DISCUSSION

A network of translesion polymerases mediates chromosomal mutagenesis.

Two decades ago, Boshoff *et al.* highlighted the importance of DnaE2 in mutagenesis, DNA damage tolerance, and pathogenicity in Mtb (Boshoff et al., 2003). Because prior attempts to deduce a function for DinBs failed to reveal any phenotype (Kana et al., 2010), DnaE2 has been considered the only mycobacterial TLS polymerase mediating chromosomal mutagenesis. However, our studies support a significant revision to this view and implicate a network of translesion polymerases in chromosomal mutagenesis.

Translesion polymerases mediate sequence specific rifampicin resistance in mycobacteria.

We confirmed published findings (Boshoff et al., 2003) showing that DnaE2 catalyzes the acquisition of rifampicin resistance in response to DNA damage. We found that DnaE2 has the ability to induce a spectrum of *rpoB* mutations, particularly S447L, S438L, H442Y, and H442D. The codons of these amino acids are conserved between *M. smegmatis* and Mtb and these mutations represent ~75% of the *rpoB* mutations detected in the sequenced rif^R Mtb clinical isolates (Tables S2, S4, and WHO mutations catalogue, 2021).

Here we report that DinB1 can induce rifampicin resistance through a mutagenic activity. In contrast to the diverse mutation spectrum of DnaE2, DinB1 confers rif^R through a unique *rpoB* mutation (CAC>CGC; H442R). This mutation has been detected in rif^R Mtb clinical isolates at a frequency between 0.8 and 5%, depending on the study (Cavusoglu et al., 2004; Hirano et al., 1999; Matsiota-Bernard et al., 1998; Qian et al., 2002; Rudeeaneksin et al., 2021; WHO mutations catalogue, 2021; Williams et al., 1998) (Tables S2 and S4). Coupled with the finding that *dinB1* expression is induced in pulmonary TB (Rachman et al., 2006), we believe that our data support shared and sequence context specific roles for DinB1 and DnaE2 in substitution mutagenesis and antibiotic resistance. This shared role raises several questions about how DinB1 and DnaE2 cooperate or compete at the replication fork. Both DinB1 and DnaE2 interact with the β clamp, DinB1 directly and DnaE2 via the ImuB protein (Gessner et al., 2021; Warner et al., 2010). Whether these two proteins compete for the same binding site, are recruited based on the type of damage, or can occupy different sites on the β clamp remains to be determined.

This work, together with the previous DnaE2 studies, suggests that TLS polymerases may be attractive drug targets to prevent the acquisition of antibiotic resistance in Mtb (Boshoff et al., 2003; Warner et al., 2010). However, we recently showed that mycobacterial TLS polymerases contribute to antibiotic bactericidal action elicited by the genomic incorporation of oxidized nucleotides when the MutT system is depleted (Dupuy et al., 2020). Thus, TLS inhibition might have salutary effects on resistance, while diminishing the bactericidal effects of some antibiotics, a balance that will need to be assessed.

DinB1 and DnaE2 as agents of frameshift mutagenesis.

In addition to its role in substitution mutagenesis, we found that DinB1 is the primary mediator of spontaneous -1 FS mutagenesis whereas DnaE2 is involved in DNA damage-induced -1 FS mutagenesis. We demonstrated that DinB1 is prone to FS in homo-oligonucleotide runs and that the FS mutagenic activity of DinB1 is conserved between *M. smegmatis* and Mtb. We observed low frequency of DinB1 slippage on homo-oligonucleotide runs in vitro, contrasting with the significant increase of -1 and +1 FS frequency measured in vivo when DinB1 is expressed. Because we found that DinB1 mutagenesis depends on its β clamp interaction, we hypothesize that slippage might be increased if the β clamp was tethering DinB1 to the template.

FS mutations are an increasingly recognized source of genomic diversity in Mtb. Mycobacterial genomes have a similar frequency of nucleotide substitutions compared to other bacteria but a higher frequency of FS mutations in homo-oligonucleotide runs (Springer et al., 2004). This can be explained by the absence of the conventional MutS/L mismatch repair in mycobacteria, functionally replaced by a NucS-dependent system which can correct substitution mutations but not indels (Castañeda-García et al., 2017, 2020). A recent in silico analysis of 5977 clinical Mtb isolates established that indels appear every 74,497 bases in genic regions and that the most common indel is -1 FS (two times more frequent than +1 FS and 6-fold more frequent than any other indel) (Gupta and Alland, 2021). These indels are significantly enriched in homo-oligonucleotide runs.

Two seminal recent studies (Bellerose et al., 2019; Safi et al., 2019) demonstrated a link between Mtb antibiotic tolerance and homo-oligonucleotide FS mutagenesis. Specifically, FS mutations in a run of 7C in the *glpK* gene, which encodes an enzyme of the glycerol metabolism, was found to control antibiotic tolerance and colony phase variation. This reversible phase variation is based on

two successive FS mutations: first a +1 FS in *glpK* conferring tolerance and second a -1 FS restoring the original open reading frame of *glpK*. Reversible gene silencing through frameshifting is not restricted to the *glpK* gene. For example, another reversible drug resistance mechanism mediated by FS in the *orn* gene has recently been reported in Mtb (Safi et al., 2020). Moreover, Gupta and Alland identified 74 events in the genome of Mtb clinical isolates designated as "frame-shift scars": two FS mutations in the same gene that disrupt and subsequently restore the integrity of the gene (Gupta and Alland, 2021). These events have been found in 48 genes of Mtb and multiple scars were detected in the ESX-1 gene cluster encoding a secretion system important for Mtb virulence. Frequent frameshifting in homo-oligonucleotide runs of the ESX-1 gene cluster of Mtb clinical isolates has also been reported (Godfroid et al., 2020). High FS incidence has also been found in PE-PPE genes (Godfroid et al., 2020; Gupta and Alland, 2021) encoding secreted proteins (Fishbein et al., 2015). The Mtb genome contains around 170 000 runs of three homo-oligonucleotides or more (Sreenu et al., 2007). We believe that our study indicates that TLS polymerases are major contributors to the mycobacterial genome plasticity and advance DinB1 and DnaE2 as the prime mediators of homo-oligonucleotide FS mutagenesis.

Redundant activities between TLS polymerases confer tolerance to alkylation damage.

In this study, we also discovered that *dinB1* and *dnaE2* have a redundant role in resistance to alkylation damage in *M. smegmatis*. The ability of DinB to confer alkylation damage tolerance has been reported in *E. coli* (Bjedov et al., 2007) and for *Pseudomonas aeruginosa* and *Pseudomonas putida*, taxa in which a DnaE2 homolog also plays a role (Jatsenko et al., 2017). Alkylation damage can be generated by exogenous and endogenous sources (Beranek, 1990; De Bont and van Larebeke, 2004). Most endogenous sources of alkylation damage in bacteria are produced by metabolic enzymes catalyzing nitrosylation (Sedgwick, 1997; Taverna and Sedgwick, 1996). Mtb is exposed to nitrosative stress during macrophage infection (Ehrt and Schnappinger, 2009; Stallings and Glickman, 2010). A recent study reported that the pathogenic bacterium *Brucella abortus* encounters alkylating stress during macrophage infection and that the alkylation-specific repair systems are required for long-term mouse infection (Poncin et al., 2019). In Mtb, the deletion of similar alkylation-specific repair systems causes sensitivity to alkylating agents but does not impact virulence (Durbach et al., 2003; Yang et al., 2011), suggesting a possible functional redundancy between alkylation-specific repair systems and the TLS polymerases. Future studies

462 will be conducted to investigate the redundancy between DnaE2, DinBs, and the alkylation-
463 specific repair systems in the tolerance to alkylation damage and Mtb survival during infection.

464 In summary, we have discovered a role of mycobacterial TLS polymerases, in particular DinB1,
465 in alkylation damage tolerance, genome plasticity, and antibiotic resistance. We believe that the
466 capability of DinB1 and DnaE2 to incorporate FS in homo-oligonucleotide runs complements
467 recent data implicating reversible gene silencing through FS mutagenesis as an important
468 mechanism of genome diversification in *M. tuberculosis* with links to antibiotic tolerance and
469 virulence.

STAR METHODS

Key resources table

REAGENT or RESOURCE	SOURCE	IDENTIFIER
Antibodies		
anti-RecA	Pocono Rabbit Farm & Laboratory	(Wipperman et al., 2018)
anti-RpoB	Biolegend	Cat#663905 RRID: AB_2566583
Bacterial and virus strains		
Mycobacterium smegmatis mc^{2}155 (Wild type)		
Wild-type	(Snapper et al., 1990)	N/A
PDS122 (Δ*dinB2*)	(Dupuy et al., 2020)	N/A
PDS139 (Δ*dnaE2*)	(Dupuy et al., 2020)	N/A
PDS353 (Δ*recA*)	(Dupuy et al., 2020)	N/A
PDS380 (Δ*dinB1*)	(Dupuy et al., 2020)	N/A
PDS382 (Δ*dinB3*)	(Dupuy et al., 2020)	N/A
PDS388 (Δ*dinB1* Δ*dinB2* Δ*dinB3*)	(Dupuy et al., 2020)	N/A
PDS394 (Δ*dnaE2* Δ*dinB1* Δ*dinB2* Δ*dinB3*)	(Dupuy et al., 2020)	N/A
PDS622 (*leuD*$^{-1}$)	This work	N/A
PDS630 (*leuD*$^{-2}$)	This work	N/A
PDS632 (*leuD*$^{-2}$ Δ*dinB2*)	This work	N/A
PDS684 (*leuD*$^{-2}$ Δ*dnaE2*)	This work	N/A
PDS686 (*leuD*$^{-2}$ Δ*dinB1*)	This work	N/A
PDS688 (*leuD*$^{-2}$ Δ*dinB3*)	This work	N/A
PDS690 (*leuD*$^{-2}$ Δ*dinB123*)	This work	N/A
PDS692 (*leuD*$^{-2}$ Δ*dnaE2*Δ*dinB2*)	This work	N/A
Escherichia coli		
E. coli DH5α (F$^-$ Φ80*lac*ZΔM15 Δ(*lac*ZYA-*arg*F) U169 *rec*A1 *end*A1 *hsd*R17(r_K^-, m_K^+) *pho*A *sup*E44 *thi*-1 *gyr*A96 *rel*A1 λ$^-$)	Lab stock	N/A
Chemicals, peptides, and recombinant proteins		
Hygromycin	Fisher scientific	Cat#10687010
Streptomycin	Thermofisher scientific	Cat#15140122
Kanamycin	Fisher scientific	Cat#AAJ1792406
Ciprofloxacin	Fisher scientific	Cat#AC449620050
Hydrogen peroxide	Fisher scientific	Cat#H325-100
Methyl methanesulfonate (MMS)	Alfa Aesar	Cat#H55120
Methylnitronitrosoguanidine (MNNG)	Pfaltz and Bauer	Cat#NC9068843
Nitrofurazone (NFZ)	Sigma-Aldrich	Cat#1465004
4-nitroquinoline-1oxide (4-NQO)	Sigma-Aldrich	Cat#N8141
Anhydrotetracycline (ATc)	Fisher scientific	Cat#AAJ66688MA
Mitomycin C (MMC)	Sigma-Aldrich	Cat#10107409001
BstB1 restriction enzyme	New England Biolabs	Cat#R0519L
Cla1 restriction enzyme	New England Biolabs	Cat#R0197L
EcoR1 restriction enzyme	New England Biolabs	Cat#R0101L
Nde1 restriction enzyme	New England Biolabs	Cat#R0111L
Phusion High Fidelity Polymerase	Fisher scientific	Cat#F530L

In-Fusion HD Cloning Kit	Takara Bio USA	Cat#639650
QIAprep Spin Miniprep Kit	Qiagen	Cat#27106
QIAquick Gel Extraction Kit	Qiagen	Cat#28706
M. smegmatis DinB1	(Ordonez et al., 2014)	N/A
Amersham ECL western blotting detection reagents	GE Healthcare	Cat#RPN2106
NuPAGE™ 4 to 12%, Bis-Tris gel	Novex	Cat#NP0336PK2
Experimental models: Organisms/strains		
M. smegmatis mc^{2}155		
Wild-type	(Snapper et al., 1990)	N/A
PDS122 (Δ*dinB2*)	(Dupuy et al., 2020)	N/A
PDS139 (Δ*dnaE2*)	(Dupuy et al., 2020)	N/A
PDS353 (Δ*recA*)	(Dupuy et al., 2020)	N/A
PDS380 (Δ*dinB1*)	(Dupuy et al., 2020)	N/A
PDS382 (Δ*dinB3*)	(Dupuy et al., 2020)	N/A
PDS388 (Δ*dinB1* Δ*dinB2* Δ*dinB3*)	(Dupuy et al., 2020)	N/A
PDS394 (Δ*dnaE2* Δ*dinB1* Δ*dinB2* Δ*dinB3*)	(Dupuy et al., 2020)	N/A
PDS622 (*leuD*$^{-1}$)	This work	N/A
PDS630 (*leuD*$^{-2}$)	This work	N/A
PDS632 (*leuD*$^{-2}$ Δ*dinB2*)	This work	N/A
PDS684 (*leuD*$^{-2}$ Δ*dnaE2*)	This work	N/A
PDS686 (*leuD*$^{-2}$ Δ*dinB1*)	This work	N/A
PDS688 (*leuD*$^{-2}$ Δ*dinB3*)	This work	N/A
PDS690 (*leuD*$^{-2}$ Δ*dinB123*)	This work	N/A
PDS692 (*leuD*$^{-2}$ Δ*dnaE2*Δ*dinB2*)	This work	N/A
Oligonucleotides		
For plasmid constructs (detailed in Table S1)		
ODP290: CAGAAAGGAGGCCATATGGAGGGCACCGTC	This work	N/A
ODP291: AGGTCGACGGTATCGCTACGGCGTGCTCTGG	This work	N/A
ODP292: AGGTCGACGGTATCGCTACTTTTCGAACTGCGGGTGGCTCCACGGCGTGCTCTGGTAG	This work	N/A
ODP293: GGCGAACGACAGCTGTTCGAGG	This work	N/A
ODP294: CAGCTGTCGTTCGCCGAGGCCTTCGGTGAACC	This work	N/A
ODP295: CAGGAACGCGTCCATGTCCAG	This work	N/A
ODP296: ATGGACGCGTTCCTGGCATCCGTCGAGCAGC	This work	N/A
ODP343: CAGAAAGGAGGCCATGTGCTGCACCTGGACATG	This work	N/A
ODP344: AGGTCGACGGTATCGTCACCGGTCGCCGAC	This work	N/A
ODP389: CTAGTATGCATCATAAGGCTTTGGCCTACATGGAC	This work	N/A
ODP390: CATCACGCTTCTCCTTCGTG	This work	N/A
ODP391: AGGAGAAGCGTGATGAGGCTTTCACCACTCACACC	This work	N/A
ODP392: CTAGGCAATTGCATATGTAGTCATCAATCCTGAACGG	This work	N/A
ODP393: AGGAGAAGCGTGATGGGCTTTCACCACTCACACC	This work	N/A
ODP425: TCCAGCTGCAGAATTATGGTGGCGTTGTACTCGG	This work	N/A
ODP426: CTTATCTGTGAATTTCTGTGAATCC	This work	N/A
ODP427: AAATTCACAGATAAGATGACCAAATGGGTGCTCCAC	This work	N/A
ODP428: GATAAGCTTCGAATTTCGAGGTTAGGTGCCTGCAG	This work	N/A
ODP429: TCCAGCTGCAGAATTTGCTGTTGTCGCTGATCGATC	This work	N/A

ODP430: GATAAGCTTCGAATTTCTTCTAGTCCGGCAGCATGG	This work	N/A
ODP433: CCGGATATCCGACAGGCCG	This work	N/A
ODP434: CTGTCGGATATCCGGCCGGACCTGGAACAACCCGAG	This work	N/A
ODP435: TCCAGCTGCAGAATTATGGCACCGTCACTGCCGAAC	This work	N/A
ODP436: GATAAGCTTCGAATTTCACCGGTCGCCGACGTC	This work	N/A
ODP437: TCCAGCTGCAGAATTACGCAATCGTGCACTCCTGTTG	This work	N/A
ODP438: GATAAGCTTCGAATTCTAGGCCAGTTCTAACCGCACTC	This work	N/A
ODP443: TCCAGCTGCAGAATTTCCCAAGGACACTGAGTCC	This work	N/A
ODP444: GATAAGCTTCGAATTTTGCTGACTCATACCAGGC	This work	N/A
ODP445: CATAACACCCCTTGTATTACTG	This work	N/A
ODP446: ACAAGGGGTGTTATGTTTAGCCATATTCAACGGGAAACG	This work	N/A
ODP447: ACAAGGGGTGTTATGCCCAGCCATATTCAACGGGAAACG	This work	N/A
ODP448: ACAAGGGGTGTTATGGGAAGCCATATTCAACGGGAAACG	This work	N/A
ODP449: ACAAGGGGTGTTATGGAAAGCCATATTCAACGGGAAACG	This work	N/A
ODP450: ACAAGGGGTGTTATGTTTTAGCCATATTCAACGGGAAACG	This work	N/A
ODP451: ACAAGGGGTGTTATGCCCCAGCCATATTCAACGGGAAACG	This work	N/A
ODP452: ACAAGGGGTGTTATGGGGAAGCCATATTCAACGGGAAACG	This work	N/A
ODP453: ACAAGGGGTGTTATGGAAAAGCCATATTCAACGGGAAACG	This work	N/A
ODP454: ACAAGGGGTGTTATGTTTTTTAGCCATATTCAACGGGAAACG	This work	N/A
ODP455: ACAAGGGGTGTTATGCCCCCCAGCCATATTCAACGGGAAACG	This work	N/A
ODP456: ACAAGGGGTGTTATGGGGGGAAGCCATATTCAACGGGAAACG	This work	N/A
ODP457: ACAAGGGGTGTTATGGAAAAAAGCCATATTCAACGGGAAACG	This work	N/A
ODP480: TCCAGCTGCAGAATTTGAGTTCGACCTCACCGTTGAC	This work	N/A
ODP481: GATAAGCTTCGAATTTCGACGTGCTGCCGGAAG	This work	N/A
ODP490: ACAAGGGGTGTTATGTTTTTAGCCATATTCAACGGGAAACG	This work	N/A
ODP491: ACAAGGGGTGTTATGCCCCCAGCCATATTCAACGGGAAACG	This work	N/A
ODP492: ACAAGGGGTGTTATGGGGGAAGCCATATTCAACGGGAAACG	This work	N/A
ODP493: ACAAGGGGTGTTATGGAAAAAGCCATATTCAACGGGAAACG	This work	N/A
ODP514: CAGAAAGGAGGCCATGTGGAGTCCCGCTGGG	This work	N/A
OAM118: GTACCAGATCTTTAAATACGATCTGGCGTGCG	This work	N/A
OAM185: CATCGATAAGCTTCACTTCTCGAACTGGGGGTGGCTCCACCGGAAGTCG CGGGAG	This work	N/A
For in vitro frameshifting assay		
SG-FS1: CGTGTCGCCCTTC	This work	N/A
SG-FS2: GGGTTTTGAAGGGCGACACG	This work	N/A
SG-FS3: GGGTTTTTTGAAGGGCGACACG	This work	N/A
SG-FS4: GGGTTTTTTTTGAAGGGCGACACG	This work	N/A
SG-FS5: CCCAAAAGAAGGGCGACAC	This work	N/A
SG-FS6: CCCAAAAAAGAAGGGCGACAC	This work	N/A
SG-FS7: CCCAAAAAAAAGAAGGGCGACAC	This work	N/A
SG-FS8: TTTCCCCGAAGGGCGACACG	This work	N/A
SG-FS9: TTTCCCCCCGAAGGGCGACACG	This work	N/A
SG-FS10: TTTCCCCCCCCGAAGGGCGACACG	This work	N/A
SG-FS11: AAAGGGGGAAGGGCGACACG	This work	N/A
SG-FS12: AAAGGGGGGGAAGGGCGACACG	This work	N/A
SG-FS13: AAAGGGGGGGGGAAGGGCGACACG	This work	N/A
For *rpoB*, *leuD*, *leuC* and *kan* mutation sequencing (PCR and sequencing primers)		
ODP378 (fw *rpoB*): CAAGAAGCTGGGCCTGAACGC	This work	N/A

ODP379 (rev *rpoB*): GCGGTTGGCGTCGTCGTG	This work	N/A
ODP380 (seq *rpoB*): GAGCGTGTCGTGCGTGAG	This work	N/A
ODP398 (fw *leuC-leuD*): ACCACGTTCGAGTTCCTCAAGG	This work	N/A
ODP395 (rev *leuC-leuD*): TTCAGGCGAAGCTAGCGAAC	This work	N/A
ODP399 (seq *leuC-leuD*): TCCAACCGCAACTTCGAGG	This work	N/A
ODP476 (fw *kan*): TGGCCTTTTGCTGGCCTTTTGC	This work	N/A
ODP477 (rev *kan*): TTCAACAAAGCCGCCGTCCC	This work	N/A
ODP479 (seq *kan*): ACTGAATCCGGTGAGAATGG	This work	N/A
Recombinant DNA		
Plasmids (cloning details in Table S1)		
pmsg419: Empty ATc-on system vector (hyg^R, OriMyc)	This work	N/A
pAJF067: Gene replacement vector (hyg^R, *galK*, sacB)	This work	N/A
pDB60: Complementation vector ($strep^R$, attP(L5))	This work	N/A
pAJF266: pMV306kan-derivative (kan^R, attP(L5), p*dnaK*)	Lab stock	(Stover et al., 1991)
pDB60-*dnaE2*: pDB60 derivative for $dnaE2^{Msm}$ complem.	This work	N/A
pDP64 : pmsg419 derivative for $dinB1^{Msm}$ expression	This work	N/A
pDP65: pmsg419 derivative for $dinB1^{ST}$ expression	This work	N/A
pDP66: pmsg419 derivative for $dinB1^{D113A\text{-}ST}$	This work	N/A
pDP67 : pmsg419 derivative for $dinB1^{F23L\text{-}ST}$	This work	N/A
pDP88: pmsg419 derivative for $dinB1^{Mtb}$ expression	This work	N/A
pDP104: pAJF067 derivative for $leuD^{\Delta 4}$ deletion ($leuD^{-1}$)	This work	N/A
pDP105: pAJF067 derivative for $leuD^{\Delta 4\text{-}5}$ deletion ($leuD^{-2}$)	This work	N/A
pDP112: pDB60 derivative for $dinB1^{Msm}$ complementation	This work	N/A
pDP114: pDB60 derivative for $dinB2^{Msm}$ complementation	This work	N/A
pDP115: pDB60 derivative for $dinB3^{Msm}$ complementation	This work	N/A
pDP117: pmsg419 derivative for $dinB1^{\Delta\beta clamp}$ expression	This work	N/A
pDP118: pDB60 derivative for $dinB1^{Mtb}$ complementation	This work	N/A
pDP119: pDB60 derivative for $dinB2^{Mtb}$ complementation	This work	N/A
pDP120: pDB60 derivative with *kan*::3T	This work	N/A
pDP121 : pDB60 derivative with *kan*::3C	This work	N/A
pDP122: pDB60 derivative with *kan*::3G	This work	N/A
pDP123: pDB60 derivative with *kan*::3A	This work	N/A
pDP124: pDB60 derivative with *kan*::4T	This work	N/A
pDP125: pDB60 derivative with *kan*::4C	This work	N/A
pDP126: pDB60 derivative with *kan*::4G	This work	N/A
pDP127: pDB60 derivative with *kan*::4A	This work	N/A
pDP128: pDB60 derivative with *kan*::6T	This work	N/A
pDP129: pDB60 derivative with *kan*::6C	This work	N/A
pDP130: pDB60 derivative with *kan*::6G	This work	N/A
pDP131: pDB60 derivative with *kan*::6A	This work	N/A
pDP144: pDB60 derivative with *kan*::5T	This work	N/A
pDP145: pDB60 derivative with *kan*::5C	This work	N/A
pDP146: pDB60 derivative with *kan*::5G	This work	N/A
pDP147: pDB60 derivative with *kan*::5A	This work	N/A
pDP157: pmsg419 derivative for $dinB1^{Mtb+5aa}$ expression	This work	N/A
Software and algorithms		
Prism 9	GraphPad	https://www.graphpad.com/

Clone manager 9	Sci Ed Software	https://www.scied.com/
Illustrator	Adobe	https://www.adobe.com/

Resource availability

Lead contact:

Further information and requests for resources and reagents should be directed to and will be fulfilled by the lead contact, Dr. Michael Glickman (Glickmam@mskcc.org).

Material availability:

Plasmids and strains generated in this study will be made available on request.

Data and code availability:

All data generated in this study are presented in the Figures and Tables. Any additional information required to reanalyze the data reported in this paper is available from the lead contact upon request.

Experimental model and subject details

Bacterial strains. Strains used in this work are listed in the key resources table. *Escherichia coli* strains were cultivated at 37°C in Luria-Bertani (LB) medium. *M. smegmatis* strains were grown at 37°C in Middlebrook 7H9 medium (Difco) supplemented with 0.5% glycerol, 0.5% dextrose, 0.1% Tween 80. Antibiotics were used at the following concentrations: 5 μg/ml streptomycin (Sm), 50 μg/ml hygromycin (Hyg).

Plasmids. Oligonucleotides and plasmids used in this study are listed in the key resources table. Details of PCR primer pairs and restriction enzymes used for each plasmid construct are detailed in Table S1. Plasmids were constructed in *E. coli* DH5α. For the construct of complementation plasmids, ORFs together with their 5' flanking regions (~500 bp) were amplified by PCR using *M. smegmatis* mc^2155 or *M. tuberculosis* Erdman genomic DNA as template. The PCR products were cloned into pDB60 digested with *EcoR1* using recombination-based cloning (In-Fusion, Takara). For the constructs of *dinB1* expression plasmids, ORFs were amplified using *M. smegmatis* mc^2155 or *M. tuberculosis* Erdman genomic DNA and were cloned into pmsg419 digested with *ClaI*. For the *leuD* inactivation plasmid construct, the ~500 bp regions flanking the deleted nucleotides were amplified using *M. smegmatis* mc^2155 genomic DNA as template and were cloned into pAJF067 digested with *Nde1* using recombination based cloning (In-Fusion,

Takara). For plasmids carrying the *kan* gene inactivated by run of homo-oligonucleotides, the *kan* gene was amplified by PCR using the pAJF266 vector as template. The amplified fragments were cloned into pDP60 digested with *EcoRI* using recombination-based cloning (In-Fusion). The absence of mutations in constructs was verified by DNA sequencing.

Method details

Construct of *M. smegmatis* strains. Plasmids were introduced into *M. smegmatis* by electrotransformation. The construct of unmarked deletion mutants used in this study is detailed in Dupuy et al., 2020. Unmarked 1 bp and 2 bp deletions upstream of the start codon of *leuD* were incorporated in each strain using a double recombination reaction as described in Barkan et al., 2011 and using plasmids listed in the key resources table and Table S1. Plasmids carrying *kan* genes inactivated by an homo-oligonucleotide run, listed in the key resources table and Table S1, were introduced at the *attB* site of the *M. smegmatis* genome.

Growth and cell viability. Cells in exponential growth phase cultured without inducer were back diluted in fresh 7H9 medium supplemented with 50 nM of inducer (Anhydrotetracycline: ATc) to OD_{600}=0.001. Growth was measured by monitoring OD_{600} for 48h. When OD_{600} reached a value around 1, cultures were back diluted in fresh +ATc 7H9 medium to OD_{600}=0.001 and measured values were multiplied by the dilution factor. For cell viability, +ATc 7H9 liquid cultures were pelleted, resuspended in –ATc 7H9 and serial dilutions were spotted and cultured on –ATc Difco Middlebrook 7H10 agar medium and incubated 48 h at 37°C. The number of CFU was counted and the result expressed in number of CFU per Optical Density Unit (ODU: CFU in 1 ml of a culture at OD_{600}=1). For growth on agar medium, cells were grown in log phase without inducer and 5 µl of serial dilutions were spotter on 7H10 medium supplemented with 0, 5 or 50 nM of ATc and incubated at 37°C for 72 h.

Disc diffusion assay. Bacteria were grown to exponential phase, diluted in 3 ml of pre-warmed top agar (7H9, 6 mg/ml agar) to an OD_{600} of 0.01 and plated on 7H10. A filter disc was put on the dried top agar and was spotted with 2.5 µl of 10 M H_2O_2, 10 mg/ml ciprofloxacin (cip), 500 µg/ml mitomycin C (MMC), 100% MMS (MMS), 100 mg/ml methylnitronitrosoguanidine (MNNG), 50 mg/ml 4-nitroquinoline 1-oxide (4-NQO), or 100 mg/ml nitrofurazone. The diameter of the growth inhibition zone was measured after incubation for 48 h at 37°C.

Agar-based assay. Bacterial cultures grown to exponential phase were diluted to an OD_{600} of 0.1. Serial dilutions were performed from 10^{0} to 10^{-5} in 7H9 and 5 µl of each dilution was plated on 7H10 or 7H10 supplemented with 0.05% MMS. Pictures were taken after 3 d incubation at 37°C.

UV sensitivity assay. Bacterial cultures in exponential growth phase were diluted to an OD_{600} of 0.1 and serial dilutions (5 µl) were spotted on 7H10 plates. The plates were exposed to UV radiation (wavelength=254 nm) at doses of 0, 5, 10, 15 or 20 J m^{-2} using a Stratalinker 2400 UV Crosslinker (Stratagene). Plates were imaged after 3 d incubation at 37°C.

Western Blot. Cell lysates were prepared from 2 ml aliquots of a log-phase culture (OD_{600} of 0.4) withdrawn at 0 h, 4 h, or 24 h after ATc addition to the cultures. Cells were pelleted, resuspended in PBS buffer supplemented with 0.1% Tween 20 (PBST), lysed by incubation with 10 mg/ml lysozyme for 15 min at 37°C, and treated with 100 mM dithiothreitol for 10 min at 95°C. Proteins were separated by electrophoresis in a NuPAGE™ 4 to 12%, Bis-Tris gel (Novex) and transferred to a PVDF membrane. Blots were blocked and probed in 5% Omniblot milk in PBST. Proteins on blots were detected using anti-RpoB or anti-RecA antibodies incubated for 1 h at 1:10,000 dilutions and secondary Horseradish peroxidase (HRP)-antibodies. Blots were imaged in iBright FL1000 (Invitrogen) after treatment of the membrane with Amersham ECL western blotting detection reagents (GE Healthcare) according to manufacturer's instructions.

Mutation frequency determination. Bacteria were grown to exponential phase in 7H9 medium from a single colony. In experiments with deletion mutants, cultures were back-diluted at an OD_{600} of 0.0005 in fresh medium and cultured for 24 h. For *dinB1* expression experiments, cultures were back diluted at OD_{600} of 0.004 in fresh medium supplemented with 50 nM ATc and cultured in presence of the inducer for 16 h. Cells (OD_{600} ~0.5) were concentrated 20-fold by centrifugation and pellet resuspension and 100 µl of a 10^{-6} dilution was plated on 7H10 agar whereas 200 µl was plated on 7H10 with 100 µg/ml rif or 4 µg/ml Kan for the measurement of substitution mutations or FS mutations in homo-oligonucleotide runs, respectively. For the measurement of FS mutations in *leuD*, cells were cultivated in 7H9 medium supplemented with 50 µg/ml leucine and plated on 7H10 (200 µl) or 7H10 supplemented with 50 µg/ml leucine. For stress-induced mutagenesis, cells were treated with UV (10 J m^{-2}) or H_2O_2 (2.5 mM) for 2 h, washed and incubated for 4 h at 37°C in fresh medium. MMS (0.010%) was added to the cultures 4 h before plating. Mutation frequency was expressed by the mean number of selected colonies per 10^{8} CFU from independent cultures.

For each strain and condition, the number of independent cultures used to measure the mutation frequency is indicated by the number of grey dots in each bar of graphs. For the determination of the mutation spectrum, the rifampicin resistance determining region (RRDR) of the *rpoB* gene in rif^R colonies, the *kan* gene in kan^R colonies or the *leuD* gene in leu^+ colonies, was amplified and sequenced using primers listed in the key resources table. Mutation spectra were expressed as relative frequency, percent of mutations types found in each strain or condition, or absolute frequency, number of mutation types per 10^8 CFU obtained by multiplying the relative frequency of the mutation by the rif^R, leu^+ or kan^R frequency.

In vitro DNA slippage assay. Recombinant *M. smegmatis* DinB1 was produced in *E. coli* and purified as described previously (Ordonez et al., 2014). Protein concentration was determined by using the Bio-Rad dye reagent with bovine serum albumin as the standard. A 5′ ^{32}P-labeled primer DNA strand was prepared by reaction of a 13-mer oligonucleotide, 5'-dCGTGTCGCCCTTC, with T4 polynucleotide kinase and [γ^{32}P]ATP. The labeled DNA was separated from free ATP by electrophoresis through a nondenaturing 18% polyacrylamide gel and then eluted from an excised gel slice. The primer-templates for assays of DNA polymerase were formed by annealing the 5′ ^{32}P-labeled 13-mer pDNA strand (SG-FS1) to a series of unlabeled template strands (SG-FS2-13) at 1:3 molar ratio to form the primer-templates depicted in Figs. 5C and S5. Polymerase reaction mixtures (10 µl) containing 50 mM Tris-HCl, pH 7.5, 5 mM $MnCl_2$, 0.125 mM dNTP or ddNTP as specified, 1 pmol (0.1 µM) ^{32}P-labeled primer-template DNA, and 10 pmol (1 µM) DinB1 were incubated at 37°C for 15 min. The reactions were quenched by adding 10 µl of 90% formamide, 50 mM EDTA, 0.01% bromophenol blue-xylene cyanol. The samples were heated at 95°C for 5 min and then analyzed by electrophoresis through a 40-cm 18% polyacrylamide gel containing 7.5 M urea in 44.5 mM Tris-borate, pH 8.3, 1 mM EDTA. The products were visualized by autoradiography. Where specified, the gel was scanned with a Typhoon FLA7000 imager and the relative distributions of individual extension products were quantified with ImageQuant software.

RT-qPCR and RNA sequencing. RT-qPCR experiments were conducted exactly as described in Adefisayo et al., 2021 whereas RNAseq results were obtained from the RNAseq raw data published in Adefisayo et al., 2021.

Quantification and statistical analysis. One-way analysis of variance (ANOVA) and a Bonferroni post-test were performed using prism9 software (GraphPad) on ln-transformed data for

all statistical analyses of this work except for growth and viability experiments for which a two-ways ANOVA was used.

ACKNOWLEDGMENTS

This work is supported by NIH (NIH grant #AI064693) and this research was funded in part through the NIH/NCI Cancer Center Support Grant P30CA008748. P. Dupuy was supported in part by a « Jeune Scientifique » salary award from the French National Institute of Agronomic Science (INRA). We thank all Glickman and Shuman lab members for helpful discussions. We thank Jamie Bean for reanalyzing the RNAseq data.–

AUTHORS CONTRIBUTIONS

P.D., S.G., O.A., S.S., and M.G. designed research; P.D., S.G., O.A., and J.B. performed research; P.D., S.G., O.A., S.S., and M.G. analyzed data; P.D. and M.G. wrote the paper, with input from S.S.

DECLARATION OF INTERESTS

MG has received consulting fees from Vedanta Biosciences, PRL NYC, and Fimbrion Therapeutics and has equity in Vedanta biosciences.

SUPPLEMENTAL INFORMATION

Figures S1-S7 and Tables S1-S4.

REFERENCES

Adefisayo, O.O., Dupuy, P., Nautiyal, A., Bean, J.M., and Glickman, M.S. (2021). Division of labor between SOS and PafBC in mycobacterial DNA repair and mutagenesis. Nucleic Acids Res. 49, 12805–12819.

Barkan, D., Stallings, C.L., and Glickman, M.S. (2011). An improved counterselectable marker system for mycobacterial recombination using galK and 2-deoxy-galactose. Gene 470, 31–36.

Bellerose, M.M., Baek, S.-H., Huang, C.-C., Moss, C.E., Koh, E.-I., Proulx, M.K., Smith, C.M., Baker, R.E., Lee, J.S., Eum, S., et al. (2019). Common Variants in the Glycerol Kinase Gene Reduce Tuberculosis Drug Efficacy. MBio 10, e00663-19.

Beranek, D.T. (1990). Distribution of methyl and ethyl adducts following alkylation with monofunctional alkylating agents. Mutat. Res. 231, 11–30.

Bjedov, I., Dasgupta, C.N., Slade, D., Le Blastier, S., Selva, M., and Matic, I. (2007). Involvement of Escherichia coli DNA polymerase IV in tolerance of cytotoxic alkylating DNA lesions in vivo. Genetics 176, 1431–1440.

Boshoff, H.I.M., Reed, M.B., Barry, C.E., and Mizrahi, V. (2003). DnaE2 polymerase contributes to in vivo survival and the emergence of drug resistance in Mycobacterium tuberculosis. Cell 113, 183–193.

Castañeda-García, A., Prieto, A.I., Rodríguez-Beltrán, J., Alonso, N., Cantillon, D., Costas, C., Pérez-Lago, L., Zegeye, E.D., Herranz, M., Plociński, P., et al. (2017). A non-canonical mismatch repair pathway in prokaryotes. Nat. Commun. 8, 14246.

Castañeda-García, A., Martín-Blecua, I., Cebrián-Sastre, E., Chiner-Oms, A., Torres-Puente, M., Comas, I., and Blázquez, J. (2020). Specificity and mutagenesis bias of the mycobacterial alternative mismatch repair analyzed by mutation accumulation studies. Sci. Adv. 6, eaay4453.

Cavusoglu, C., Karaca-Derici, Y., and Bilgic, A. (2004). In-vitro activity of rifabutin against rifampicin-resistant Mycobacterium tuberculosis isolates with known rpoB mutations. Clin. Microbiol. Infect. Off. Publ. Eur. Soc. Clin. Microbiol. Infect. Dis. 10, 662–665.

Cole, S.T., Brosch, R., Parkhill, J., Garnier, T., Churcher, C., Harris, D., Gordon, S.V., Eiglmeier, K., Gas, S., Barry, C.E., et al. (1998). Deciphering the biology of Mycobacterium tuberculosis from the complete genome sequence. Nature 393, 537–544.

Courcelle, C.T., Belle, J.J., and Courcelle, J. (2005). Nucleotide excision repair or polymerase V-mediated lesion bypass can act to restore UV-arrested replication forks in Escherichia coli. J. Bacteriol. 187, 6953–6961.

Courcelle, J., Khodursky, A., Peter, B., Brown, P.O., and Hanawalt, P.C. (2001). Comparative gene expression profiles following UV exposure in wild-type and SOS-deficient Escherichia coli. Genetics 158, 41–64.

639 Darwin, K.H., and Nathan, C.F. (2005). Role for Nucleotide Excision Repair in Virulence of
640 Mycobacterium tuberculosis. Infect. Immun. 73, 4581–4587.

641 De Bont, R., and van Larebeke, N. (2004). Endogenous DNA damage in humans: a review of
642 quantitative data. Mutagenesis 19, 169–185.

643 Dupuy, P., Howlader, M., and Glickman, M.S. (2020). A multilayered repair system protects the
644 mycobacterial chromosome from endogenous and antibiotic-induced oxidative damage. Proc.
645 Natl. Acad. Sci. 117, 19517–19527.

646 Durbach, S.I., Springer, B., Machowski, E.E., North, R.J., Papavinasasundaram, K.G., Colston,
647 M.J., Böttger, E.C., and Mizrahi, V. (2003). DNA Alkylation Damage as a Sensor of Nitrosative
648 Stress in Mycobacterium tuberculosis. Infect. Immun. 71, 997–1000.

649 Ehrt, S., and Schnappinger, D. (2009). Mycobacterial survival strategies in the phagosome:
650 defence against host stresses. Cell. Microbiol. 11, 1170–1178.

651 Erill, I., Campoy, S., Mazon, G., and Barbé, J. (2006). Dispersal and regulation of an adaptive
652 mutagenesis cassette in the bacteria domain. Nucleic Acids Res. 34, 66–77.

653 Fishbein, S., van Wyk, N., Warren, R.M., and Sampson, S.L. (2015). Phylogeny to function:
654 PE/PPE protein evolution and impact on Mycobacterium tuberculosis pathogenicity. Mol.
655 Microbiol. 96, 901–916.

656 Fuchs, R.P., and Fujii, S. (2013). Translesion DNA synthesis and mutagenesis in prokaryotes.
657 Cold Spring Harb. Perspect. Biol. 5, a012682.

658 Fujii, S., and Fuchs, R.P. (2020). A Comprehensive View of Translesion Synthesis in
659 Escherichia coli. Microbiol. Mol. Biol. Rev. MMBR 84, e00002-20.

660 Gessner, S., Martin, Z., Reiche, M.A., Santos, J.A., Dhar, N., Dinkele, R., Wet, T.D., Ramudzuli,
661 A., Anoosheh, S., Lang, D.M., et al. (2021). The mycobacterial mutasome: composition and
662 recruitment in live cells. 2021.11.16.468908.

663 Gillespie, S.H. (2002). Evolution of drug resistance in Mycobacterium tuberculosis: clinical and
664 molecular perspective. Antimicrob. Agents Chemother. 46, 267–274.

665 Godfroid, M., Dagan, T., Merker, M., Kohl, T.A., Diel, R., Maurer, F.P., Niemann, S., and
666 Kupczok, A. (2020). Insertion and deletion evolution reflects antibiotics selection pressure in a
667 Mycobacterium tuberculosis outbreak. PLoS Pathog. 16, e1008357.

668 Gupta, A., and Alland, D. (2021). Reversible gene silencing through frameshift indels and
669 frameshift scars provide adaptive plasticity for Mycobacterium tuberculosis. Nat. Commun. 12,
670 4702.

671 Hirano, K., Abe, C., and Takahashi, M. (1999). Mutations in the rpoB Gene of Rifampin-
672 Resistant Mycobacterium tuberculosis Strains Isolated Mostly in Asian Countries and Their
673 Rapid Detection by Line Probe Assay. J. Clin. Microbiol. 37, 2663–2666.

674 Houghton, J., Townsend, C., Williams, A.R., Rodgers, A., Rand, L., Walker, K.B., Böttger, E.C.,
675 Springer, B., and Davis, E.O. (2012). Important Role for Mycobacterium tuberculosis UvrD1 in
676 Pathogenesis and Persistence apart from Its Function in Nucleotide Excision Repair. J. Bacteriol.

677 Jarosz, D.F., Godoy, V.G., Delaney, J.C., Essigmann, J.M., and Walker, G.C. (2006). A single
678 amino acid governs enhanced activity of DinB DNA polymerases on damaged templates. Nature
679 439, 225–228.

680 Jatsenko, T., Sidorenko, J., Saumaa, S., and Kivisaar, M. (2017). DNA Polymerases ImuC and
681 DinB Are Involved in DNA Alkylation Damage Tolerance in Pseudomonas aeruginosa and
682 Pseudomonas putida. PloS One 12, e0170719.

683 Kana, B.D., Abrahams, G.L., Sung, N., Warner, D.F., Gordhan, B.G., Machowski, E.E.,
684 Tsenova, L., Sacchettini, J.C., Stoker, N.G., Kaplan, G., et al. (2010). Role of the DinB
685 Homologs Rv1537 and Rv3056 in Mycobacterium tuberculosis. J. Bacteriol. 192, 2220–2227.

686 Kato, T., and Nakano, E. (1981). Effects of the umuC36 mutation on ultraviolet-radiation-
687 induced base-change and frameshift mutations in Escherichia coli. Mutat. Res. 83, 307–319.

688 Kim, S.-R., Maenhaut-Michel, G., Yamada, M., Yamamoto, Y., Matsui, K., Sofuni, T., Nohmi,
689 T., and Ohmori, H. (1997). Multiple pathways for SOS-induced mutagenesis in Escherichia coli:
690 An overexpression of dinB/dinP results in strongly enhancing mutagenesis in the absence of any
691 exogenous treatment to damage DNA. Proc. Natl. Acad. Sci. U. S. A. 94, 13792–13797.

692 Kim, S.R., Matsui, K., Yamada, M., Gruz, P., and Nohmi, T. (2001). Roles of chromosomal and
693 episomal dinB genes encoding DNA pol IV in targeted and untargeted mutagenesis in
694 Escherichia coli. Mol. Genet. Genomics MGG 266, 207–215.

695 Matsiota-Bernard, P., Vrioni, G., and Marinis, E. (1998). Characterization of rpoB Mutations in
696 Rifampin-Resistant Clinical Mycobacterium tuberculosisIsolates from Greece. J. Clin.
697 Microbiol.

698 Napolitano, R., Janel-Bintz, R., Wagner, J., and Fuchs, R.P.P. (2000). All three SOS-inducible
699 DNA polymerases (Pol II, Pol IV and Pol V) are involved in induced mutagenesis. EMBO J. 19,
700 6259–6265.

701 Nathan, C., and Barry, C.E. (2015). TB drug development: immunology at the table. Immunol.
702 Rev. 264, 308–318.

703 Naz, S., Dabral, S., Nagarajan, S.N., Arora, D., Singh, L.V., Kumar, P., Singh, Y., Kumar, D.,
704 Varshney, U., and Nandicoori, V.K. (2021). Compromised base excision repair pathway in
705 Mycobacterium tuberculosis imparts superior adaptability in the host. PLoS Pathog. 17,
706 e1009452.

707 Ordonez, H., and Shuman, S. (2014). Mycobacterium smegmatis DinB2 misincorporates
708 deoxyribonucleotides and ribonucleotides during templated synthesis and lesion bypass. Nucleic
709 Acids Res. 42, 12722–12734.

710 Ordonez, H., Uson, M.L., and Shuman, S. (2014). Characterization of three mycobacterial DinB
711 (DNA polymerase IV) paralogs highlights DinB2 as naturally adept at ribonucleotide
712 incorporation. Nucleic Acids Res. 42, 11056–11070.

713 Poncin, K., Roba, A., Jimmidi, R., Potemberg, G., Fioravanti, A., Francis, N., Willemart, K.,
714 Zeippen, N., Machelart, A., Biondi, E.G., et al. (2019). Occurrence and repair of alkylating stress
715 in the intracellular pathogen Brucella abortus. Nat. Commun. 10, 4847.

716 Qian, L., Abe, C., Lin, T.-P., Yu, M.-C., Cho, S.-N., Wang, S., and Douglas, J.T. (2002). rpoB
717 genotypes of Mycobacterium tuberculosis Beijing family isolates from East Asian countries. J.
718 Clin. Microbiol. 40, 1091–1094.

719 Rachman, H., Strong, M., Ulrichs, T., Grode, L., Schuchhardt, J., Mollenkopf, H., Kosmiadi,
720 G.A., Eisenberg, D., and Kaufmann, S.H.E. (2006). Unique transcriptome signature of
721 Mycobacterium tuberculosis in pulmonary tuberculosis. Infect. Immun. 74, 1233–1242.

722 Reuven, N.B., Arad, G., Maor-Shoshani, A., and Livneh, Z. (1999). The Mutagenesis Protein
723 UmuC Is a DNA Polymerase Activated by UmuD′, RecA, and SSB and Is Specialized for
724 Translesion Replication *. J. Biol. Chem. 274, 31763–31766.

725 Rock, J.M., Lang, U.F., Chase, M.R., Ford, C.B., Gerrick, E.R., Gawande, R., Coscolla, M.,
726 Gagneux, S., Fortune, S.M., and Lamers, M.H. (2015). DNA replication fidelity in
727 Mycobacterium tuberculosis is mediated by an ancestral prokaryotic proofreader. Nat. Genet. 47,
728 677–681.

729 Rudeeaneksin, J., Phetsuksiri, B., Nakajima, C., Bunchoo, S., Suthum, K., Tipkrua, N.,
730 Fukushima, Y., and Suzuki, Y. (2021). Drug-resistant Mycobacterium tuberculosis and its
731 genotypes isolated from an outbreak in western Thailand. Trans. R. Soc. Trop. Med. Hyg. 115,
732 886–895.

733 Safi, H., Gopal, P., Lingaraju, S., Ma, S., Levine, C., Dartois, V., Yee, M., Li, L., Blanc, L., Ho
734 Liang, H.-P., et al. (2019). Phase variation in Mycobacterium tuberculosis glpK produces
735 transiently heritable drug tolerance. Proc. Natl. Acad. Sci. U. S. A. 116, 19665–19674.

736 Safi, H., Lingaraju, S., Ma, S., Husain, S., Hoque, M., Soteropoulos, P., Rustad, T., Sherman,
737 D.R., and Alland, D. (2020). Rapidly Correcting Frameshift Mutations in the Mycobacterium
738 tuberculosis orn Gene Produce Reversible Ethambutol Resistance and Small-Colony-Variant
739 Morphology. Antimicrob. Agents Chemother. 64, e00213-20.

740 Sale, J.E. (2013). Translesion DNA Synthesis and Mutagenesis in Eukaryotes. Cold Spring Harb.
741 Perspect. Biol. 5, a012708.

742 Sedgwick, B. (1997). Nitrosated peptides and polyamines as endogenous mutagens in O6-
743 alkylguanine-DNA alkyltransferase deficient cells. Carcinogenesis 18, 1561–1567.

744 Snapper, S.B., Melton, R.E., Mustafa, S., Kieser, T., and Jacobs, W.R. (1990). Isolation and
745 characterization of efficient plasmid transformation mutants of Mycobacterium smegmatis. Mol.
746 Microbiol. 4, 1911–1919.

747 Springer, B., Sander, P., Sedlacek, L., Hardt, W.-D., Mizrahi, V., Schär, P., and Böttger, E.C.
748 (2004). Lack of mismatch correction facilitates genome evolution in mycobacteria. Mol.
749 Microbiol. 53, 1601–1609.

750 Sreenu, V.B., Kumar, P., Nagaraju, J., and Nagarajam, H.A. (2007). Simple sequence repeats in
751 mycobacterial genomes. J. Biosci. 32, 3–15.

752 Stallings, C.L., and Glickman, M.S. (2010). Is Mycobacterium tuberculosis stressed out? A
753 critical assessment of the genetic evidence. Microbes Infect. Inst. Pasteur 12, 1091–1101.

754 Steinborn, G. (1978). Uvm mutants of Escherichia coli K12 deficient in UV mutagenesis. I.
755 Isolation of uvm mutants and their phenotypical characterization in DNA repair and
756 mutagenesis. Mol. Gen. Genet. MGG 165, 87–93.

757 Stover, C.K., de la Cruz, V.F., Fuerst, T.R., Burlein, J.E., Benson, L.A., Bennett, L.T., Bansal,
758 G.P., Young, J.F., Lee, M.H., and Hatfull, G.F. (1991). New use of BCG for recombinant
759 vaccines. Nature 351, 456–460.

760 Tang, M., Shen, X., Frank, E.G., O'Donnell, M., Woodgate, R., and Goodman, M.F. (1999).
761 UmuD′2C is an error-prone DNA polymerase, Escherichia coli pol V. Proc. Natl. Acad. Sci. 96,
762 8919–8924.

763 Taverna, P., and Sedgwick, B. (1996). Generation of an endogenous DNA-methylating agent by
764 nitrosation in Escherichia coli. J. Bacteriol. 178, 5105–5111.

765 Timinskas, K., and Venclovas, Č. (2019). New insights into the structures and interactions of
766 bacterial Y-family DNA polymerases. Nucleic Acids Res. 47, 4393–4405.

767 Vaisman, A., and Woodgate, R. (2017). Translesion DNA polymerases in eukaryotes: what
768 makes them tick? Crit. Rev. Biochem. Mol. Biol. 52, 274–303.

769 Wagner, J., and Nohmi, T. (2000). Escherichia coli DNA polymerase IV mutator activity:
770 genetic requirements and mutational specificity. J. Bacteriol. 182, 4587–4595.

771 Wagner, J., Gruz, P., Kim, S.R., Yamada, M., Matsui, K., Fuchs, R.P., and Nohmi, T. (1999).
772 The dinB gene encodes a novel E. coli DNA polymerase, DNA pol IV, involved in mutagenesis.
773 Mol. Cell 4, 281–286.

774 Warner, D.F., Ndwandwe, D.E., Abrahams, G.L., Kana, B.D., Machowski, E.E., Venclovas, C.,
775 and Mizrahi, V. (2010). Essential roles for imuA'- and imuB-encoded accessory factors in
776 DnaE2-dependent mutagenesis in Mycobacterium tuberculosis. Proc. Natl. Acad. Sci. U. S. A.
777 107, 13093–13098.

778 WHO (2021). Global tuberculosis report 2021.

779 WHO mutations catalogue (2021). Catalogue of mutations in Mycobacterium tuberculosis
780 complex and their association with drug resistance.

781 Williams, D.L., Spring, L., Collins, L., Miller, L.P., Heifets, L.B., Gangadharam, P.R.J., and
782 Gillis, T.P. (1998). Contribution of rpoB Mutations to Development of Rifamycin Cross-
783 Resistance in Mycobacterium tuberculosis. Antimicrob. Agents Chemother. 42, 1853–1857.

784 Wipperman, M.F., Heaton, B.E., Nautiyal, A., Adefisayo, O., Evans, H., Gupta, R., van
785 Ditmarsch, D., Soni, R., Hendrickson, R., Johnson, J., et al. (2018). Mycobacterial Mutagenesis
786 and Drug Resistance Are Controlled by Phosphorylation- and Cardiolipin-Mediated Inhibition of
787 the RecA Coprotease. Mol. Cell 72, 152-161.e7.

788 Yang, M., Aamodt, R.M., Dalhus, B., Balasingham, S., Helle, I., Andersen, P., Tønjum, T.,
789 Alseth, I., Rognes, T., and Bjørås, M. (2011). The ada operon of Mycobacterium tuberculosis
790 encodes two DNA methyltransferases for inducible repair of DNA alkylation damage. DNA
791 Repair 10, 595–602.

792 Yeiser, B., Pepper, E.D., Goodman, M.F., and Finkel, S.E. (2002). SOS-induced DNA
793 polymerases enhance long-term survival and evolutionary fitness. Proc. Natl. Acad. Sci. U. S. A.
794 99, 8737–8741.

795

Figure 1. DinB1 competes with the replicative polymerase for interaction with the β clamp at the replication fork. Growth (A, D, and G) and viability (B and F) of strains carrying an inducible (tet=Anhydrotetracycline inducible promoter) DinB1 or its indicated derivates (Msm=*M. smegmatis*, Mtb=annotated *M. tuberculosis* DinB1, Mtb+5aa=N terminal extended DinB1, *dinB1* D113A=catalytically inactive *M. smegmatis* DinB1, Δβ clamp (ΔQESLF: 356-360 amino acids of *M. smegmatis* DinB1)) in presence of inducer. The viability in (F) was measured 24 h after inducer addition. (C) Anti-RecA/RpoB immunoblot from indicated strains with indicated times of inducer treatment. (E) Alignment of Msm and Mtb DinB1 N-termini with the potential start codons underlined. The blue boxed valine corresponds to the start codon of the published DinB1 noted as $DinB1^{Mtb}$ above, whereas the red boxed valine shows an alternative start codon of an extended DinB1 denoted as $DinB1^{Mtb+5aa}$. Results shown are means (± SEM) of biological triplicates (A, B, D, and G) or from biological replicates symbolized by grey dots (F). Stars above or under the means mark a statistical difference with the reference strain (empty vector) and lines connecting two strains show a statistical difference between them (*, $P<0.05$; **, $P<0.01$; ***, $P<0.001$).

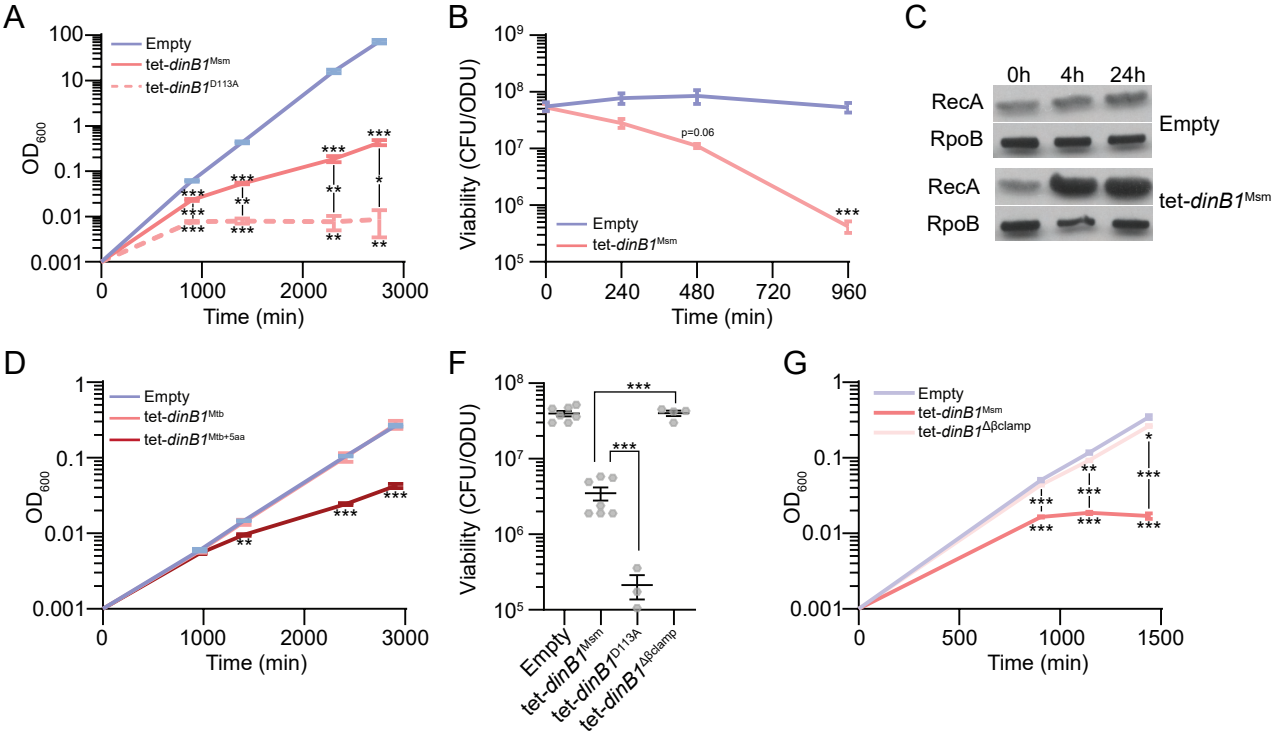

E

GGT ATG GAG GGC ACC GTC GCT CGG ACC GCG AGC CGC AGA TGG GTC CTG CAT CTG GAC ATG GAC >>>
..G ..M ..E ..G ..T ..V ..A ..R ..T ..A ..S ..R ..R ..W ..V ..L ..H ..L ..D ..M ..D >>> *dinB1*Msm

TCG GTA GCC CCA AAT AGC ATC ACG GGT GTG GAG TCC CGC TGG GTG CTG CAC CTG GAC ATG GAT >>>
..S ..V ..A ..P ..N ..S ..I ..T ..G ..V ..E ..S ..R ..W ..V ..L ..H ..L ..D ..M ..D >>> *dinB1*Mtb

Figure 1. DinB1 competes with the replicative polymerase for interaction with the β clamp at the replication fork.

Figure 2. DinB1 is an error prone polymerase inducing antibiotic resistance through a characteristic mutagenic signature. (A) Rifampicin resistance (rif^R) frequency in indicated strains in presence of inducer. Results shown are means (± SEM) of data obtained from biological replicates symbolized by grey dots. Stars above bars mark a statistical difference with the reference strain (empty vector) and lines connecting two strains show a statistical difference between them (***, P<0.001). (B) Relative (pie chart) and absolute (bar chart) frequencies of nucleotide changes detected in *rpoB* of indicated strains rif^R. The number of sequenced rif^R is given in the center of each pie chart. (C) Location and relative frequency in % of mutated nucleotides in *rpoB* found in empty (blue), tet-*dinB1*^{Msm} (red) or tet-*dinB1*^{Mtb} (orange) rif^R. (D) Absolute frequency of the main *rpoB* mutations found in indicated strains.

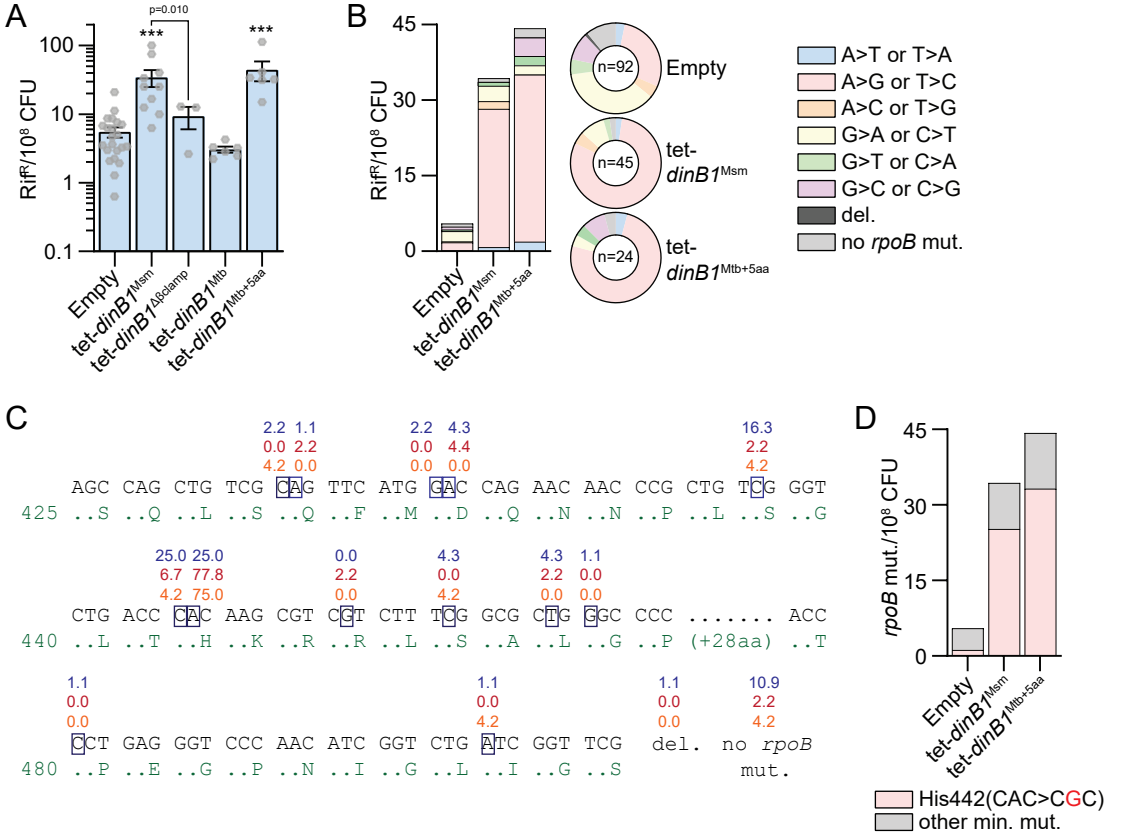

Figure 2. DinB1 is an error prone polymerase inducing antibiotic resistance through a characteristic mutagenic signature.

Figure 3. DnaE2 but not DinBs mediates stress-induced substitution mutagenesis. (A) Rifampicin resistance (rif^R) frequency in indicated strains and conditions. Results shown are means (± SEM) of data obtained from biological replicates symbolized by grey dots. Stars above bars mark a statistical difference with the reference strain (WT of each condition) (*, $P<0.05$; **, $P<0.01$). (B) Relative (pie chart) and absolute (bar chart) frequencies of nucleotide changes detected in *rpoB* of indicated strains rif^R. The number of sequenced rif^R is given in the center of each pie chart. (C) Location and relative frequency of mutated nucleotides of *rpoB* found in rif^R of Δ*dnaE2*+H_2O_2 (orange) or WT+H_2O_2 (red). The bar chart shows the absolute frequency of the main *rpoB* mutations found in indicated strains.

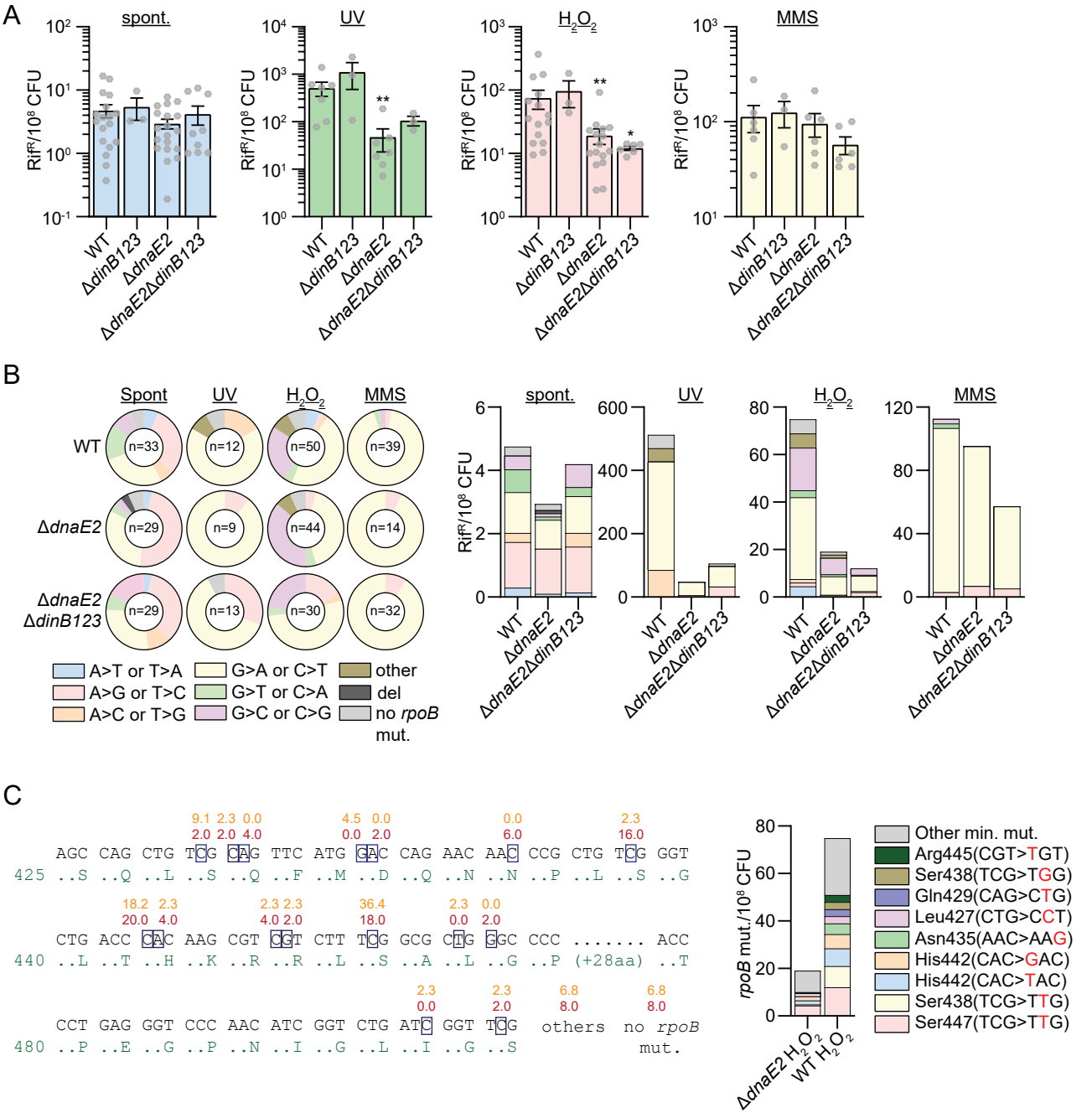

Figure 3. DnaE2 but not DinBs mediates stress-induced substitution mutagenesis.

Figure 4. Redundancy of DinB1 and DnaE2 in tolerance to alkylation damage. Sensitivities of indicated strains to indicated alkylating agents measured by disc diffusion assay. Results shown are means (± SEM) of data obtained from biological replicates symbolized by grey dots. Stars above the means mark a statistical difference with the reference strain (WT or Δ*dnaE2* Δ*dinB123*+empty in complementation experiments) (*, P<0.05; **, P<0.01; ***, P<0.001).

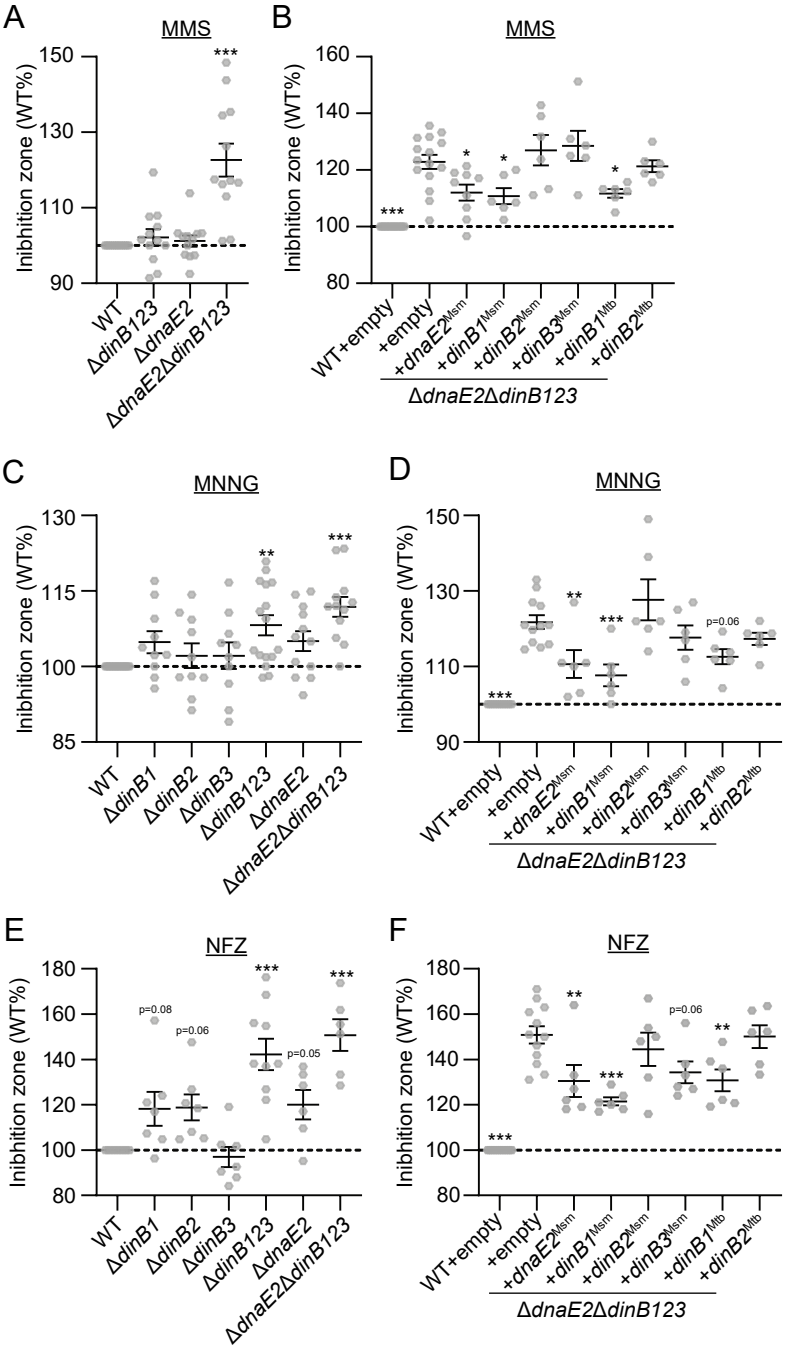

Figure 4. Redundancy of DinB1 and DnaE2 in tolerance to alkylation damage.

Figure 5. DinB1 promotes -1 and +1 frameshift mutations in homo-oligonucleotide runs. (A) *leuD* and *kan* frameshift (FS) reporter assays. *leuD* and *kan* open reading frame N-termini in which 2 base pairs in the second *leuD* codon were removed (blue box) or 4T/5T runs (red box) were incorporated upstream the start codon of *kan*. Reversion can occur by FS mutations that restore the *leuD* or *kan* reading frames resulting in phenotypic leucine prototrophy (leu^+) or kanamycin resistance (kan^R). The red box in *leuD* shows the run of 3T in which the majority of detected FS in leu^+ were found. (B) leu^+ and (C and D) kan^R frequencies in the indicated strains in presence of inducer. Results shown are means (± SEM) of data obtained from biological replicates symbolized by grey dots. Stars above the means mark a statistical difference with the reference strain (empty) (*, $P<0.05$; ***, $P<0.001$). Relative (pie chart) and absolute (bar chart) frequencies of nucleotide changes detected in *leuD* of leu^+ cells or in *kan* of kan^R cells represented with colors: red=-1 FS in the 3T run (B), 4T run (C), or 5T run (D), other colors=FS outside of the run, and grey=no detected mutation. The number of sequenced leu^+ or kan^R colonies is given in the center of each pie chart. (E) DinB1 polymerase reaction mixtures containing 5' ^{32}P-labeled primer-template DNAs with A4, A6, A8, T4, T6, or T8 runs in the template strand (depicted below and included as indicated above the lanes) and 125 μM deoxynucleotides and dideoxynucleotides (as specified above the lanes) were incubated at 37˚C for 15 min. DinB1 was omitted from reactions in lanes –. The reaction products were analyzed by urea-PAGE and visualized by autoradiography. The +1 slippage products are indicated.

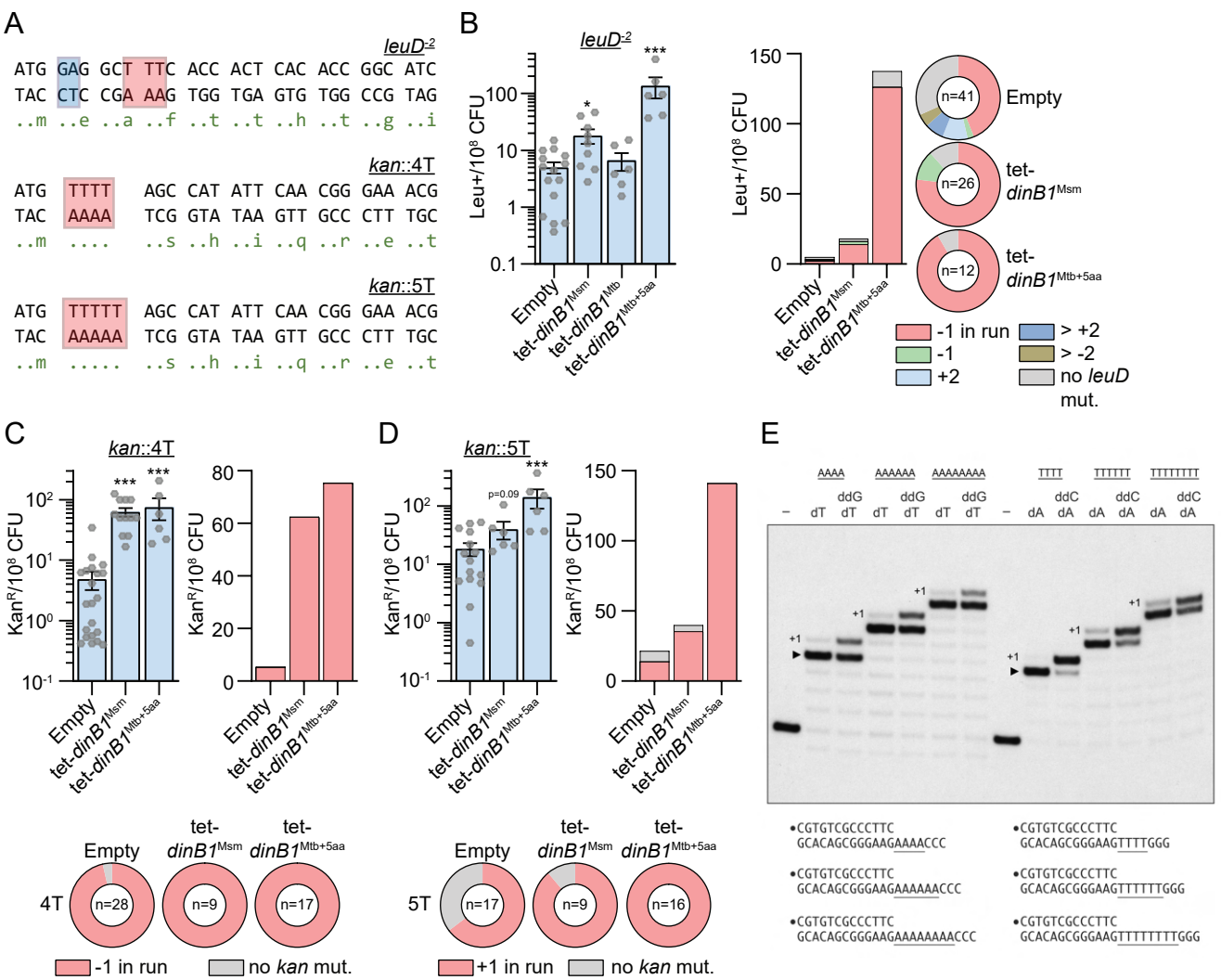

Figure 5. DinB1 promotes -1 and +1 frameshift mutations in homo-oligonucleotide runs.

Figure 6. DinB1 is the primary mediator of spontaneous -1 frameshift mutations in homo-oligonucleotide runs. (A and B) leu^+ or (C) kan^R frequency in the indicated strains and relative (pie chart) or absolute (bar chart) frequencies of nucleotide changes detected in *leuD* or *kan* coded by color. The number of sequenced leu^+ or kan^R colonies is given in the center of each pie chart. Results shown are means (± SEM) of data obtained from biological replicates symbolized by grey dots. Stars above bars mark a statistical difference with the reference strain (WT) and lines connecting two strains show a statistical difference between them (*, $P<0.05$; **, $P<0.01$; ***, $P<0.001$).

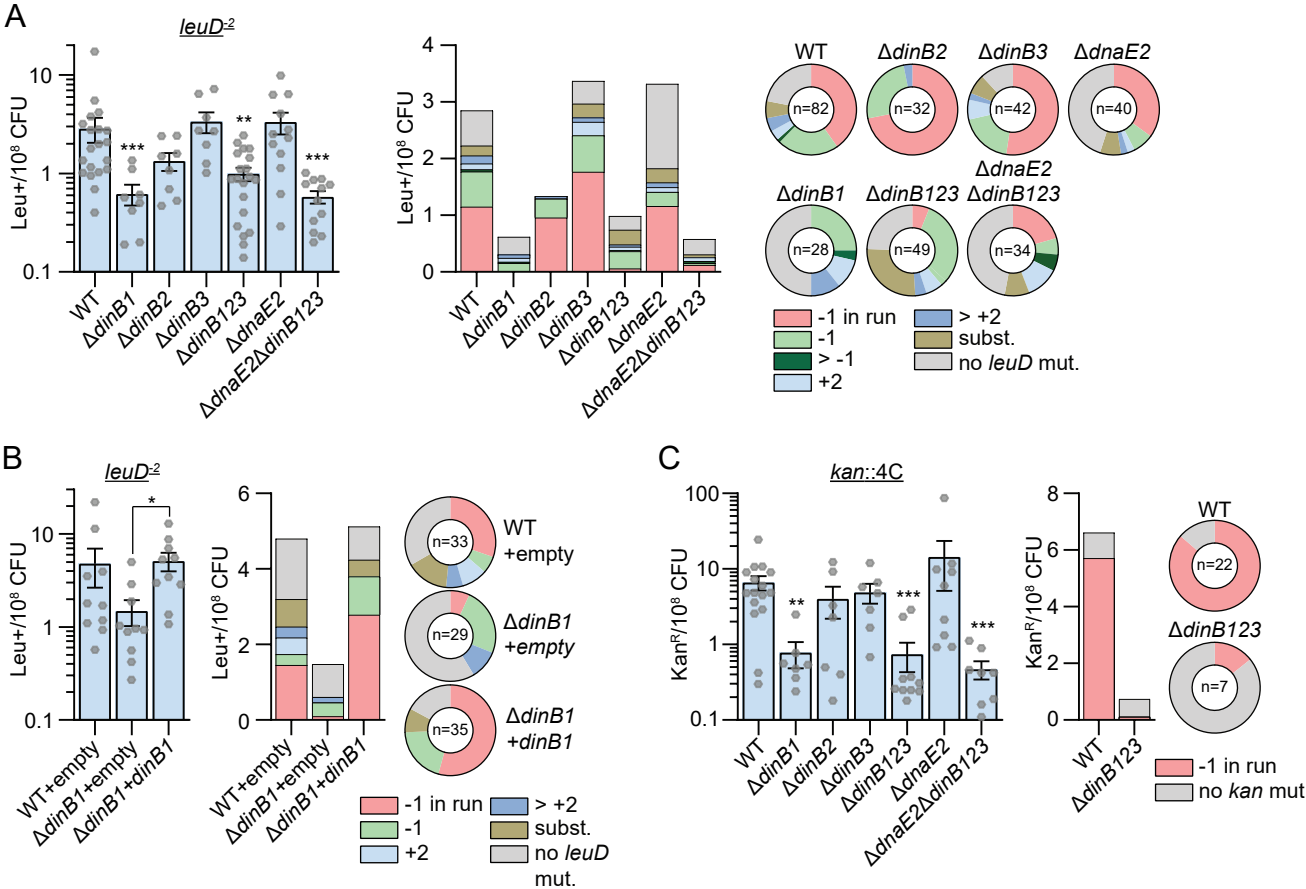

Figure 6. DinB1 is the primary mediator of spontaneous -1 frameshift mutations in homo-oligonucleotide runs.

Figure 7. DnaE2 is the primary mediator of DNA damage-induced -1 frameshift mutations in homo-oligonucleotide runs. (A) leu^+ or (B) kan^R frequency in indicated strains/conditions and relative (pie chart) or absolute (bar chart) frequencies of nucleotide changes detected in *leuD* or *kan* coded by color. The number of sequenced leu^+ or kan^R colonies is given in the center of each pie chart. Results shown are means (± SEM) of data obtained from biological replicates symbolized by grey dots. Stars above bars mark a statistical difference with the reference strain (WT+UV) and lines connecting two strains show a statistical difference between them (*, $P<0.05$; **, $P<0.01$; ***, $P<0.001$).

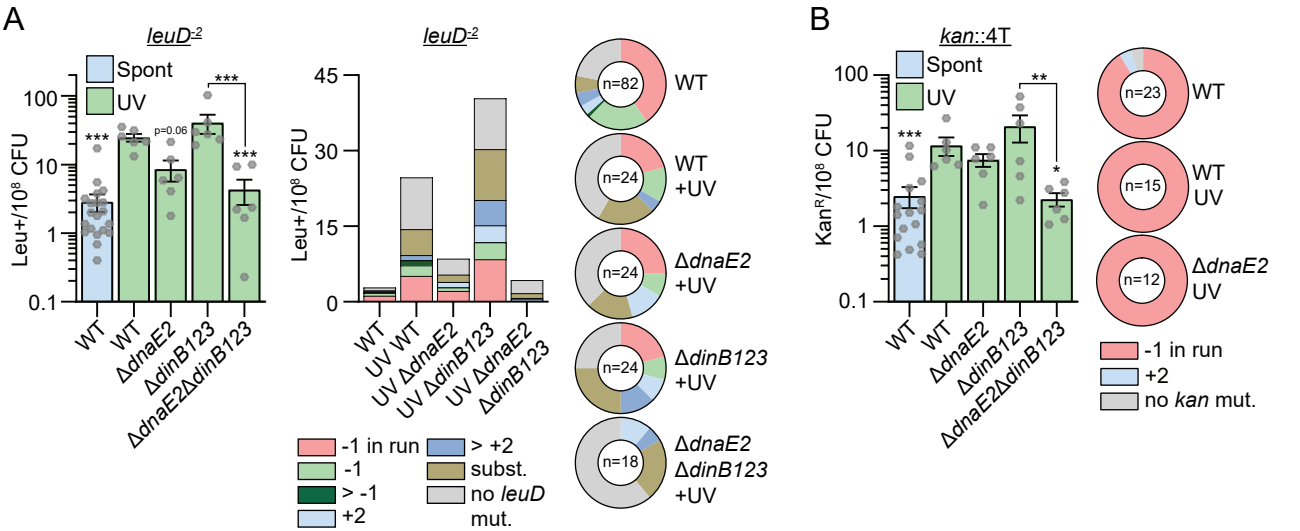

Figure 7. DnaE2 is the primary mediator of DNA damage-induced -1 frameshift mutations in homo-oligonucleotide runs.